Journal of Mammalogy, 103(6):1259–1277, 2022
https://doi.org/10.1093/jmammal/gyac057
Version of Record, first published online August 18, 2022, with fixed content and layout in compliance with Art. 8.1.3.2 ICZN.

A new genus and species of shrew-like mouse (Rodentia: Muridae) from a new center of endemism in eastern Mindanao, Philippines

Dakota M. Rowsey,[1,6,*] Mariano Roy M. Duya,[2] Jayson C. Ibañez,[3] Sharon A. Jansa,[4] Eric A. Rickart,[5] and Lawrence R. Heaney[1]

[1]*Field Museum of Natural History, 1400 S Lake Shore Drive, Chicago, Illinois 60605, USA*
[2]*Institute of Biology, University of the Philippines–Diliman, Quezon City 1101, Philippines*
[3]*Philippine Eagle Foundation, Philippine Eagle Center, Malagos, Baguio District Davao City 8000, Philippines*
[4]*Department of Ecology, Evolution, and Behavior, University of Minnesota, 140 Gortner Laboratory, 1479 Gortner Avenue, St. Paul, Minnesota 55108, USA*
[5]*Natural History Museum of Utah, University of Utah, Salt Lake City, Utah 84108, USA*
[6]*Present address: Arizona State University Natural History Collections, 734 W Alameda Drive, Tempe, Arizona 85282, USA*

**To whom correspondence should be addressed: drowsey@asu.edu*

The Philippine archipelago hosts an exceptional diversity of murid rodents that have diversified following several independent colonization events. Here, we report the discovery of a new species of rodent from Mt. Kampalili on eastern Mindanao Island. Molecular and craniodental analyses reveal this species as a member of a Philippine "New Endemic" clade consisting of *Tarsomys*, *Limnomys*, and *Rattus everetti* (tribe Rattini). This new species of "shrew-mouse" is easily distinguished from its relatives in both craniodental and external characteristics including a long, narrow snout; small eyes and ears; short, dark, dense fur dorsally and ventrally; stout body with a tapering, visibly haired tail shorter than head and body length; stout forepaws; bulbous and nearly smooth braincase; narrow, tapering rostrum; short incisive foramina; slender mandible; and narrow, slightly opisthodont incisors. This new genus and species of murid rodent illustrates that murids of the tribe Rattini have exhibited greater species and morphological diversification within the Philippines than previously known and provides evidence that Mt. Kampalili represents a previously unrecognized center of mammalian endemism on Mindanao Island that is deserving of conservation action.

Key words: biogeography, conservation, diversification, endemism, montane forest, mossy forest, Mt. Kampalili, oceanic island, taxonomy

Nomenclatural statement: A Life Science Identifier (LSID) number was obtained for this publication: urn:lsid:zoobank.org:pub:7F40AE93-8338-4745-8C75-D101E9A4F7BA

Oceanic archipelagos and their constituent islands are often hotspots of biological endemism due to their geological dynamism, relative isolation, and elevational habitat heterogeneity (Wallace 1880; Valente et al. 2014; Steinbauer et al. 2016; Whittaker et al. 2017; Veron et al. 2019). This endemism is often accompanied by morphological diversification and ecological specialization reminiscent of a classical adaptive radiation through ecological opportunity (Gillespie 2004; Givnish et al. 2009; Mahler et al. 2010). The murid rodents of the Indo-Australian archipelago provide excellent support for the notion that islands promote lineage and morphological diversification, with rodent assemblages on islands of both continental and oceanic origins exhibiting multiple instances of colonization and subsequent in situ speciation (e.g., Jansa et al. 2006; Schenk et al. 2013; Rowe et al. 2019).

The native murid rodents of the Philippine archipelago comprise a particularly striking example of a species- and endemism-rich fauna, resulting from multiple colonization events with varying degrees of ecological specialization among lineages: with 79 currently described endemic murid rodent species and several undescribed species, it is one of the richest rodent diversity hotspots in the world, with species that range over more than two orders of magnitude in body weight and including hard-seed specialists to earthworm and arthropod

specialists (Heaney et al. 2009, 2016b, 2021; Rickart et al. 2019). Despite sustained efforts to characterize its biodiversity, the Philippines remains an area of predicted underrepresentation of total vertebrate species diversity, including mammals (Moura and Jetz 2021). The diversity of this system likely owes much to the lengthy and complex geological history and diverse topography of the Philippines, characterized by dynamic tectonic shifts, volcanism, and fluctuating sea levels (Yumul et al. 2008; Mines and Geosciences Bureau 2010; Hall 2013) that together promote ecological diversification and repeated dispersal within and between islands in the archipelago (Heaney 1986; Jansa et al. 2006; Justiniano et al. 2015; Kyriazis et al. 2017; Heaney et al. 2018; Rowsey et al. 2018).

In this paper, we report the discovery of a new species of shrew-like mouse from Mt. Kampalili in the eastern highlands of Mindanao Island, Philippines (Fig. 1). Detailed craniodental and phylogenetic analyses reveal that the Kampalili shrew-mouse is a member of the Philippine endemic clade of the tribe Rattini that includes *Tarsomys*, *Limnomys*, and *Rattus everetti* (subsequently referred to as the *Tarsomys* clade), a group that is most diverse on Mindanao. This murine rodent is remarkable in that it outwardly resembles the Philippine "shrew-mice" of the genera *Archboldomys* and *Soricomys* which are members of the tribe Chrotomyini (sensu Rowsey et al. 2018) and are restricted to Luzon Island, as well as *Crunomys*, a member of the tribe Rattini that also resembles shrews and occurs on Mindanao and Luzon as well as Sulawesi (Musser 1982a; Achmadi et al. 2013). This resemblance is based on the following traits (Fig. 2): small body size, a slender and elongated snout with narrow incisors, small eyes, short ears, a stout body with a tapering tail considerably shorter than the length of head and body, short and dense fur that is dark in color dorsally and

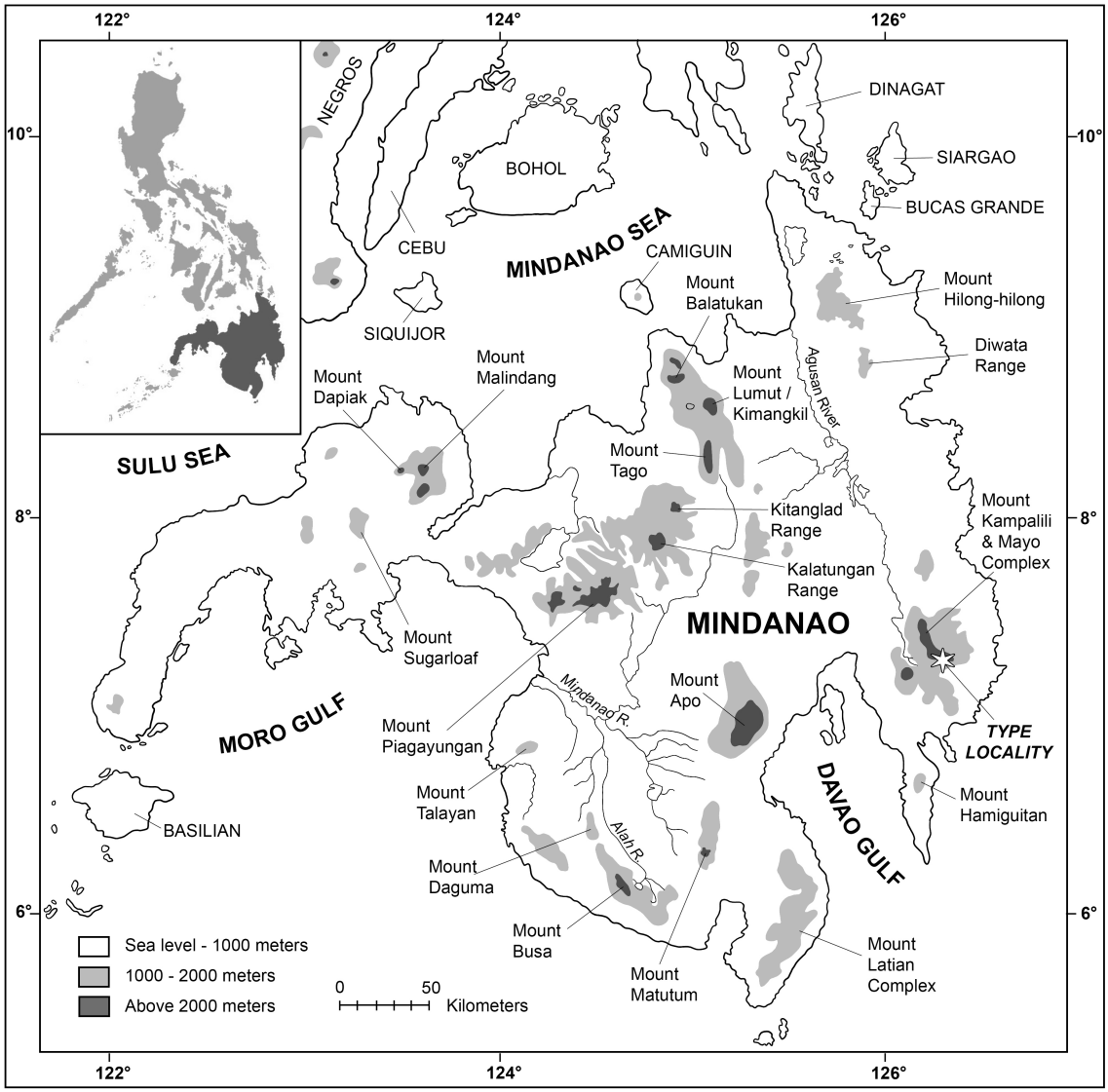

Fig. 1.—Map of Mindanao and adjacent islands in the southern Philippines showing geographic features referred to in the text, and the type locality of the new species (white star). Inset shows the location of Mindanao within the Philippines.

Fig. 2.—*Baletemys kampalili*. Illustration by Velizar Simeonovski, based on FMNH 208788, holotype.

ventrally, robust forepaws, a shallow and slender mandible, a smooth and inflated braincase, and short incisive foramina that terminate anterior to the first upper molar. We describe the Kampalili mouse as a new genus and species and discuss the implications of its discovery for mammalian biogeography and conservation in eastern Mindanao.

Materials and Methods

Specimens sampled for use in this study are deposited in the Field Museum of Natural History (FMNH), supplemented by sequence data obtained from tissue specimens deposited in the University of Kansas Natural History Museum (KU), the University of California, Berkeley Museum of Vertebrate Zoology (MVZ), the Museums Victoria (NMV), the University of Michigan Museum of Zoology (UMMZ), the Australian Biological Tissue Collection (ABTC) of the South Australian Museum (SAM), and the Museum Zoologicum Bogoriense (MZB). All fieldwork was conducted in accordance with pertinent Philippine laws and regulations; scientific study permits were granted by the Philippine Department of Environment and Natural Resources. Animals used in this study were handled in accordance with field guidelines and best practices established by the American Society of Mammalogists (Sikes et al. 2016). We sampled specimens from several other murine lineages to evaluate species relationships from phenetic and phylogenetic perspectives. Two of these species, *Tarsomys echinatus* and an undescribed *Tarsomys* species from Mt. Kampalili, are important to include in comparison to the new species, but our ability to draw definitive conclusions with respect to interspecific differences is limited as only one specimen was available for each of these.

DNA sequencing and molecular phylogenetic analysis.—We sampled members of Phloeomyini (sensu Lecompte et al. 2008), Chrotomyini, and Rattini totaling 149 individuals representing 53 species, both to determine the degree of phylogenetic divergence of the new species from its closest relatives as well as to understand its evolutionary history in the context of other lineages endemic to Southeast Asia, including other radiations in the Philippines. In total, we generated 298 new sequences with supplementary sequences acquired from GenBank (Appendix; Supplementary Data SD1).

We sequenced seven loci: mitochondrial gene cytochrome *b* (Cytb; 1,144 bp), nuclear intron 7 of beta-fibrinogen (Fgb7; 840 bp), intron 3 of opsin (Opn, an X-linked locus; 1,547 bp), exon 10 of growth hormone receptor (Ghr; 915 bp), exon 1 of interphotoreceptor retinoid binding protein (Rbp3; 1,434 bp), a portion of the single exon of recombination activating gene 1 (Rag1; 2,097 bp), and portions of exons 1 and 2 of acrosin spanning the intervening intron (Acr; 1,125 bp) for a total sequence alignment length of 9,102 bp (Supplementary Data SD3). Newly extracted DNA for this study originated from tissues of vouchered specimens held at FMNH. DNA was extracted using a QIAGEN DNeasy Blood and Tissue Kit (Germantown, Maryland). We amplified all loci using polymerase chain reaction (PCR) conditions optimized for each locus. For PCR protocols and primers used, see Supplementary Data SD2. All molecular protocols were performed in the Field Museum Pritzker Molecular Laboratory. Sequence reads were assembled in Geneious R10 (Biomatters Ltd, Auckland, New Zealand). Some specimens exhibited length heterozygotes for Fgb7, Opn, and Acr reads. For these individuals we phased the haplotypes using Indelligent (Dmitriev and Rakitov 2008) and generated a consensus sequence from these single-direction reads before assembling them with the other read direction. Consensus sequences from the resulting read assemblies, along with consensus sequences obtained from GenBank, were aligned for each locus using MUSCLE (Edgar 2004), with additional adjustments made by eye, and concatenated for subsequent analysis. All newly generated sequences have been submitted to GenBank under accession numbers OM502569–OM502864. We detected no alignment-ambiguous regions that were necessary to exclude from the analysis. Our alignment is available in Supplementary Data SD3.

The concatenated alignment was analyzed using PartitionFinder v. 2.1.1 (Lanfear et al. 2012) to determine the best-fitting nucleotide substitution models. For RAxML (Stamatakis et al. 2008) we ran the analysis with a partitioned General Time Reversible model with invariant sites, gamma-distributed rate heterogeneity, and estimated initial base frequencies (Gu et al. 1995). We specified three putative candidate partitions for each exon and one for each intron. For *BEAST (Ogilvie et al. 2017), we instead performed model fitting with one candidate partition for each exon and one for each intron using all nucleotide substitution models supported by *BEAST. In both analyses, partitioning schemes were compared using the Bayesian Information Criterion (BIC; Schwarz 1978). The resultant nucleotide partitioning scheme for each analysis can be found in Supplementary Data SD4.

We inferred evolutionary relationships for the concatenated sequence alignment under maximum likelihood (ML) using the RAxML-HPC v.8 workflow on the CIPRES Science Gateway (Stamatakis et al. 2008; Miller et al. 2010) with nodal support

inferred from 1,000 bootstrap replicates using both the full data set as well as for nuclear loci only (Supplementary Data SD5). We performed a Bayesian species tree analysis using *BEAST v. 2.6.0, also implemented in CIPRES (Miller et al. 2010; Bouckaert et al. 2014, 2019; Ogilvie et al. 2017). To calibrate this analysis in absolute time, we used secondary calibration points from a previous study (Rowsey et al. 2018, based on fossil data from Kimura et al. 2015) to specify normal clade age priors for Phloeomyini (mean: 11.1 Ma, standard deviation: 0.825), Chrotomyini (mean: 7.22 Ma, standard deviation: 0.506), and Rattini (mean: 8.82 Ma, standard deviation: 0.66). We specified nucleotide substitution models according to the PartitionFinder best-fit scheme and modeled separate molecular clocks for Cytb and the nuclear loci. We specified a relaxed lognormal molecular clock for Cytb (Drummond et al. 2006), but a strict molecular clock for the nuclear partitions to facilitate Markov-Chain Monte Carlo optimizer convergence. We additionally specified a Yule branching model (Yule 1924) with an exponential prior and a "linear with constant root" coalescence model with a population mean described by a 1/X prior with a mean of 1.0. All other priors were given default values. The full analysis was performed using three independent runs for a total of 7.5×10^9 generations with 9,800 samples and 4,900 trees retained after burn-in. We generated a maximum clade credibility (MCC) tree using TreeAnnotator v.2.6.0, specifying the nodal ages of this tree calculated based on the median clade ages of the tree distribution.

Morphometric data collection and analysis.—For evaluating species recognition from a phenetic standpoint, we sampled at least eight individuals (when available) from members of the genera *Limnomys* and *Tarsomys,* plus *R. everetti* based on their phylogenetic proximity to the new species (specimens examined listed in Appendix). When possible, we included individuals from these species collected from the same mountain (Mt. Kampalili) as the putative new species. We measured adults based on (i) fusion of the sutures between the basisphenoid and the presphenoid and basioccipital bones and (ii) complete eruption of and signs of wear on all molars. In total, we sampled 39 individuals including the two adult specimens of the new species. Linear measurements, in millimeters, including total length (TOT), tail length (LT), hindfoot length including claws (HF), ear notch length (EAR), and weight in grams (WT) were taken in the field. Combined head and body length (HBL) was determined by subtraction of tail length from total length. We measured fur length at mid-dorsum (LOF) and tail scale rings per centimeter at one-third tail length (TSR) from a subset of these specimens after fixation in formalin followed by transfer to 70% ethanol. Finally, we collected 18 craniodental measurements defined by Musser and Heaney (1992): basioccipital length (BOL), interorbital breadth (IB), zygomatic breadth (ZB), mastoid breadth (MB), length of nasal bones (LN), length of incisive foramina (LIF), depth of rostrum (DR), length of rostrum (LR), orbitotemporal length (OL), crown length of maxillary molar toothrow (LM1–3), labial palatal breadth at M^1 (PBM1), length of diastema (LD), post-palatal length (PPL), lingual palatal breadth at M^3 (PBM3), height of braincase (HBC), breadth of M^1 (BM1), breadth of incisors at tip (BIT), and breadth of zygomatic plate (BZP). These measurements were chosen based on their ability to discriminate among cryptic murine species (Heaney et al. 2011, 2014, 2021; Balete et al. 2012, 2015). The right side of the skull was measured unless the structure was damaged on the right side of the skull only; in this case, the left side was measured. All cranial measurements were taken by D. M. Rowsey using a digital caliper calibrated to 0.01 mm (Supplementary Data SD6). Measurement error was estimated by measuring three specimens of different sizes five times each, calculating the coefficient of variation for each measurement, and averaging the coefficient of variation across the three specimens. Defined as such, measurement error averages 2% and is less than 4% for all measurements (mean: 0.021, range: 0.0092–0.036).

We collected summary statistics of external, cranial, and dental measurements, including mean, standard deviation, and range using the R statistical software program v. 3.5.1 (R Core Team 2018). We pooled measurements for males and females due to limited sample sizes for most species, although available evidence suggests minimal sexual dimorphism in at least one species in the *Tarsomys* clade (Heaney et al. 2006). We assessed quantitative phenetic variation in craniodental morphology by performing a principal component analysis (PCA) on the correlation matrix of our natural-log-transformed measurements from adult specimens. We followed Brown (1972) and Brown and Yalden (1973) for terminology for external anatomy, and Musser and Heaney (1992) for cranial anatomy and dental characters.

Results

Molecular phylogenetic analysis.—The best-fit nucleotide partition model for the ML inference supported six partitions (Supplementary Data SD3). The resulting tree (Fig. 3) provides strong support for the monophyly of the three major murid clades sampled: Phloeomyini, Chrotomyini, and Rattini. However, although nodal support within Rattini is variable, our analysis shows the genus *Rattus* to be paraphyletic with respect to *R. everetti*, as recovered by several previous studies (Jansa et al. 2006; Schenk et al. 2013; Rowe et al. 2019), which exhibits a close relationship to *Tarsomys*, *Limnomys*, the Kampalili shrew-mouse, and an undescribed rat endemic to Sibuyan Island, Philippines. We note that *Rattus* (sensu stricto, defined as the clade containing *R. rattus*) is also paraphyletic with respect to Sahulian (Australian, New Guinean, and Melanesian) members assigned to this genus (e.g., *R. praetor* and *R. novaeguineae*), though support for this paraphyly is weak (Fig. 3). Although the monophyly of the Sahulian clade is strongly supported, as in previous analyses (Rowe et al. 2011, 2019), our analysis largely fails to provide support for interspecific relationships within this clade. We note also that we recovered very strong support for *Palawanomys furvus* nested within *Rattus* (sensu stricto), with a close relationship to *R. tiomanicus* and *R. mindorensis* (Fig. 3). Clearly, the problematic and unresolved relationships among "*Rattus*" species remains an important, if challenging, issue that warrants further research.

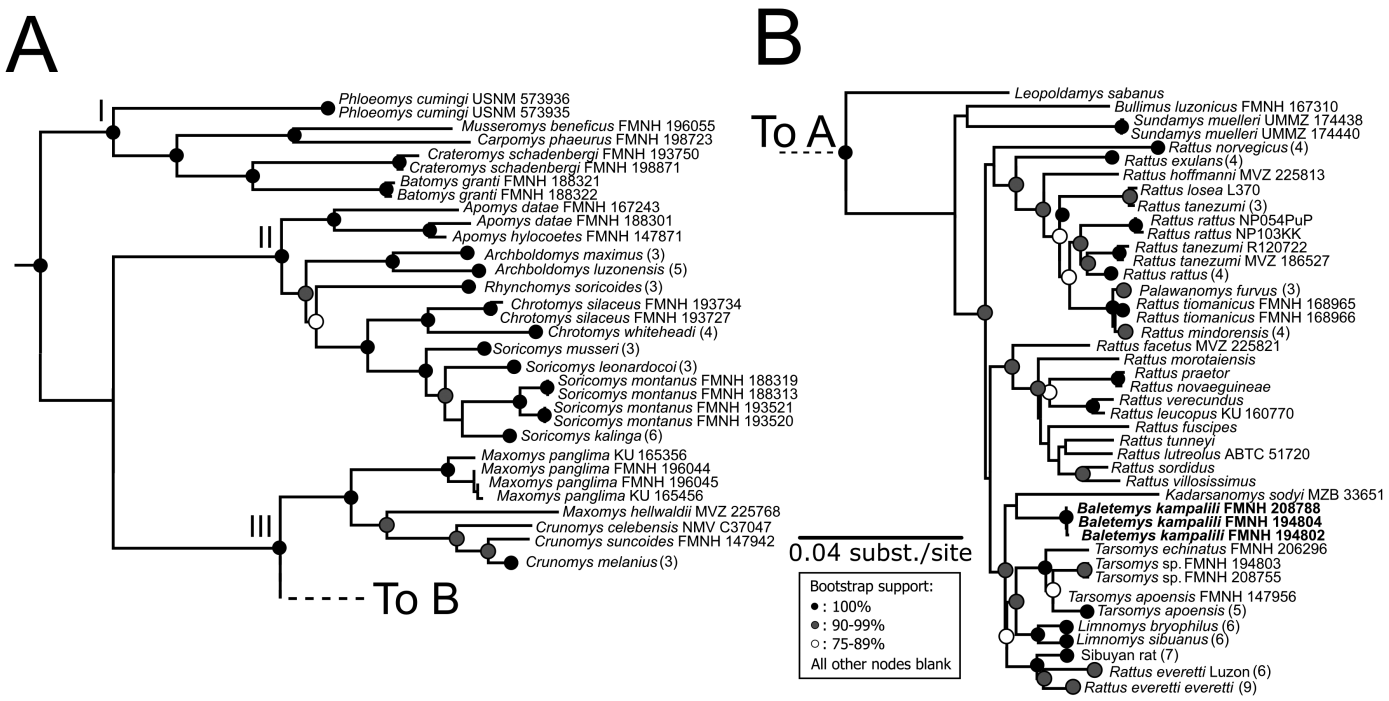

Fig. 3.—Maximum likelihood phylogenetic tree generated from multilocus concatenated sequence data. Branch lengths are proportional to number of nucleotide substitutions. Dots at nodes indicate bootstrap support. Individuals within species with strong nodal support have been collapsed when three or more individuals have been sampled, with the number sampled in parentheses after the species name.

Relationships among members of the *Tarsomys* clade in the ML analysis are somewhat uncertain given our molecular sampling. The ML topology illustrates a sister relationship between the new species and the Javan endemic *Kadarsanomys sodyi* but without bootstrap support (ML BS = 24%). We were unable to obtain a voucher for morphometric data or additional sequence data from this species to verify this placement. We recovered only moderate support for the monophyly of the *Tarsomys* clade (ML BS = 77%) to the exclusion of the Kampalili shrew-mouse. Other relationships within the *Tarsomys* clade (Fig. 3) were much more strongly supported, including the sister relationship between *Tarsomys* and *Limnomys* (ML BS = 98%) as well as between *R. everetti* and the undescribed rat from Sibuyan Island (recorded by Heaney et al. (1998) as "*Tarsomys* sp. A"; ML BS = 100%). We recovered strong support for the monophyly of *Tarsomys apoensis*, with the exception of one individual (FMNH 147956), in which the ML topology rendered the species monophyletic but with low support. This specimen was the only sample for which we were unable to amplify Cytb and the placement of this specimen in this analysis may be an artifact of missing data. To examine this, we repeated the ML analysis excluding Cytb and recovered similar results in most areas of the tree, albeit with lower support throughout (Supplementary Data SD5). In the specific case of the relationships among species in the genus *Tarsomys*, excluding Cytb obfuscates any support for the relationship between *T. apoensis* and Mt. Kampalili *Tarsomys* sp. (Supplementary Data SD5), suggesting that the sampled nuclear loci lack resolution at this scale.

The recovered topology differs between our ML (Fig. 3) and Bayesian (Fig. 4) analyses with respect to the placement of the new species. We recovered strong support for the monophyly of the *Tarsomys* clade in this analysis, including the new species. However, the placement of the new species as sister to any other lineage within the *Tarsomys* clade is not supported; its placement as sister to the unnamed Sibuyan Island rat and *R. everetti* received little support (PP = 0.37). Corroborating our ML results, we recovered strong support for the sister relationship between *R. everetti* and the unnamed Sibuyan Island rat as well as between *Limnomys* and *Tarsomys*. The *Tarsomys* clade was recovered as sister to *K. sodyi* but without support (PP = 0.66; Fig. 4).

Divergence date estimates among these taxa indicate that the diversification of the currently described genera of the *Tarsomys* clade likely occurred within the past 2.5 million years. Most species in this clade have diverged from their nearest sister species between 1 and 2 Ma, consistent with estimates of colonization and diversification within the Philippines that have been reported previously for other Philippine Rattini (Fig. 4; Jansa et al. 2006; Kyriazis et al. 2017; Rowsey et al. 2018).

Morphometric analysis.—Crania of genera included in the *Tarsomys* clade differ visibly in size, proportional length and robustness of rostrum, shape of the braincase, and many more features (Fig. 5). We conducted a PCA of the correlation matrix of log-transformed linear measurements of the cranium and teeth to quantitatively document the distinctiveness of the new species from its closest relatives (Fig. 6). PC1 accounts for 93.25% of data set variance and has low but similar positive factor loadings for all variables, primarily reflecting variation

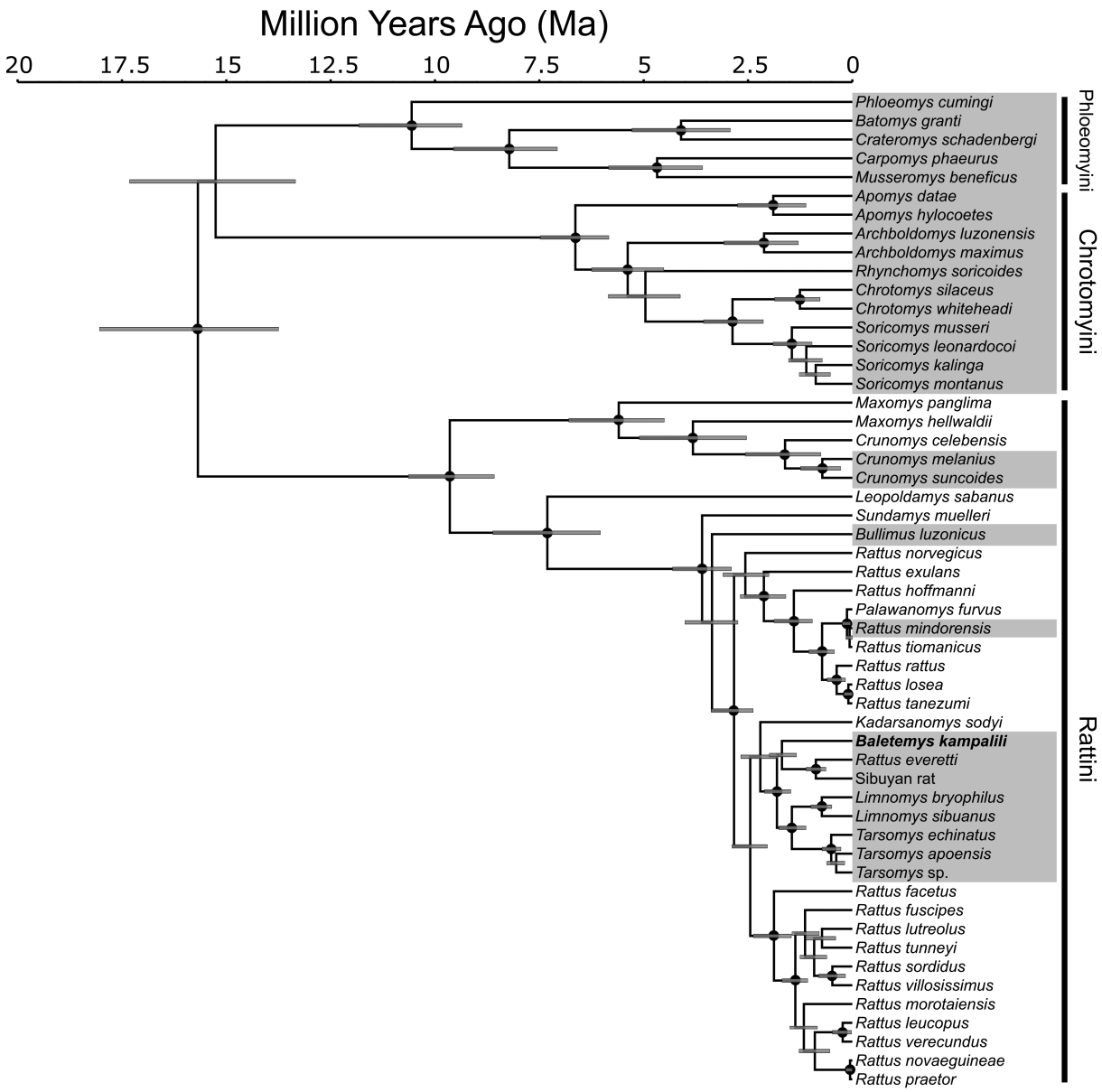

Fig. 4.—Time-calibrated maximum clade credibility (MCC) tree from Bayesian species tree analysis. The phylogeny was calibrated based on the crown ages of Phloeomyini, Chrotomyini, and Rattini inferred by previous studies (Aghová et al. 2018; Rowsey et al. 2018). Dots at nodes indicate posterior probability for the indicated relationship ≥ 0.95. Gray bars at nodes indicate 95% highest posterior density interval of divergence dates. Boxed taxa are endemic to the oceanic Philippines (i.e., excluding biogeographically distinct islands such as Palawan and other islands of the western Philippines that are located on the Sunda Shelf).

among specimens due to size and associated allometric effects (Table 1). The variance explained by this axis is noteworthy in its magnitude and suggests that size and shape of *Tarsomys*-clade murines are highly correlated. Along this axis, the new species overlaps with *L. bryophilus* but is smaller than all three species of *Tarsomys*, corroborating size similarities and differences among specimens as measured by HBL (Table 2) but also indicating other similarities in skull form correlated with size. PC2 and PC3 account for 2.22% and 1.39% of data set variance, respectively (Table 1), but results on these component axes must be interpreted with caution because their eigenvalues are small (<1.0). PC2 is influenced primarily by the shape of the palate and narrowness of the incisors, with high-scoring individuals having long, wide posterior palates and narrow incisors. On this axis the two Kampalili mouse specimens differ from one another due to one specimen having a proportionally shorter basicranium, narrower palate, and narrower incisors. PC3 loads most heavily for the length of the incisive foramen, the width of the first molar, and the width of the molar rows, with low-scoring individuals having a wide interorbit, short incisive foramina, a large M1, and long molar row. The Kampalili shrew-mouse has the lowest scores on PC3, indicating a shorter incisive foramen, a broader first molar, and a longer molar row than its close relatives (Fig. 5B).

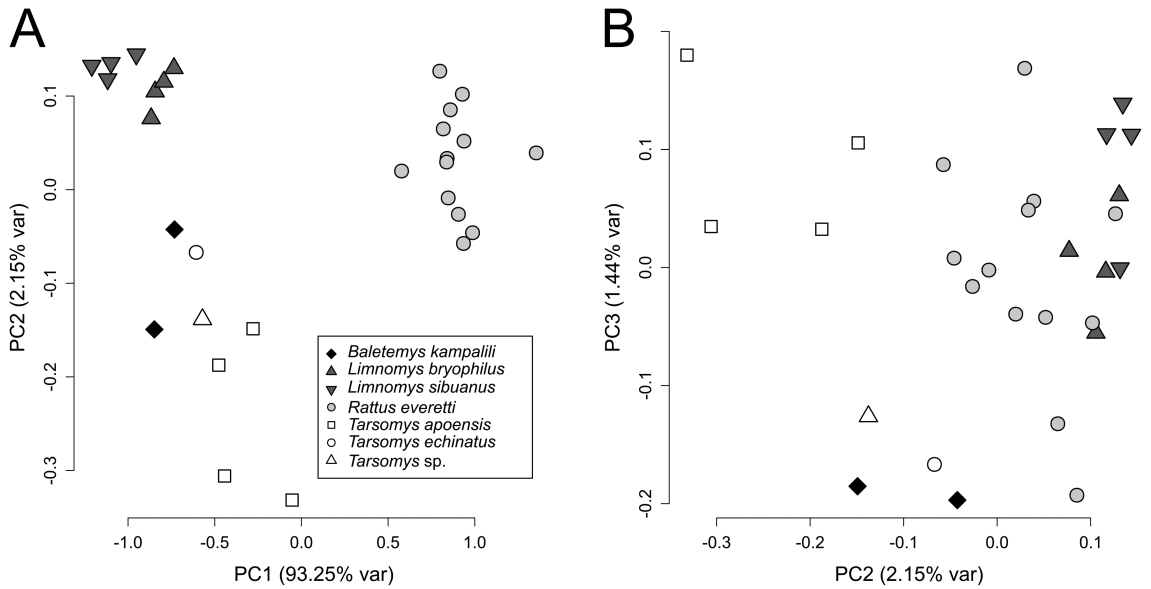

Fig. 5.—Principal component analysis of log-transformed linear skull measurements. (A) Plot of PC1 and PC2; (B) plot of PC2 and PC3. See Table 1 for component loadings.

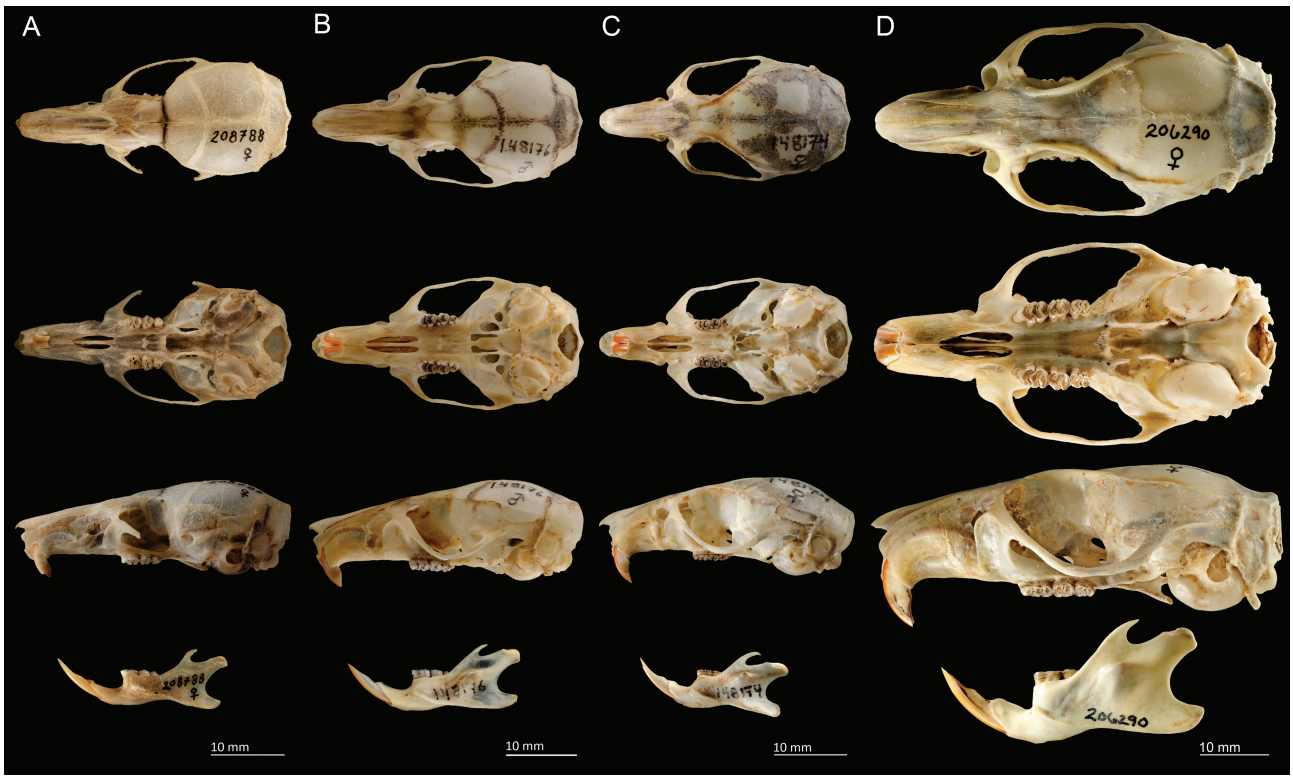

Fig. 6.—Dorsal, ventral, and lateral views of (A) *Baletemys kampalili* FMNH 208788 compared to (B) *Tarsomys apoensis* FMNH 148176, (C) *Limnomys sibuanus* FMNH 148174, and (D) *Rattus everetti* FMNH 206290. Approximately life size.

We conclude that the combination of phylogenetic and morphometric distinctiveness, along with other gross morphological diagnostic features and geographic isolation (described below), strongly indicate that this shrew-mouse from Mt. Kampalili in eastern Mindanao, Philippines is a distinct genus and species on the basis of phylogenetic relationships, branch lengths, and external and cranial morphology.

Baletemys, new genus

Type species.—*Baletemys kampalili*, new species described below.

Etymology.—We combine the Greek "*mys*" (mouse) with "Balete," in honor of the late Danilo S. Balete, whose extensive contributions to understanding Philippine biodiversity,

Table 1.—Summary table, eigenvalues, and loadings for principal component analysis of *Baletemys*- and *Tarsomys*-clade cranial linear morphometrics.

	PC1	PC2	PC3	PC4
Standard deviation	0.859	0.130	0.107	0.0862
Proportion of variance	0.933	0.02	0.014	0.0094
Cumulative proportion	0.933	0.954	0.969	0.978
Eigenvalue	14.847	0.377	0.235	0.151
Loading	PC1	PC2	PC3	PC4
BOL	0.272	0.027	–0.027	0.130
IB	0.188	–0.231	–0.341	0.339
MB	0.156	–0.040	–0.021	0.081
LN	0.267	–0.135	–0.072	0.280
LIF	0.266	–0.121	0.610	–0.231
DR	0.282	0.195	0.005	0.206
LR	0.255	–0.239	–0.145	0.201
OL	0.257	0.287	0.140	–0.134
LM1-3	0.320	0.009	–0.280	–0.432
PBM1	0.212	–0.310	–0.122	–0.244
LD	0.260	–0.137	–0.001	0.253
PPL	0.223	0.401	0.043	0.281
PBM3	0.228	–0.508	0.387	–0.023
HBC	0.162	0.193	–0.115	0.053
BM1	0.250	0.022	–0.403	–0.482
BIT	0.327	0.402	0.210	–0.064
BZP	0.272	0.027	–0.027	0.130

Table 2.—List of external measurements for selected *Tarsomys*-clade rodents, including the new genus and species, given in the form mean ± 1 *SD* followed by ranges. Numbers in parentheses indicate the number of individuals sampled for that measurement if less than the *n* for each species given in the column heading.

	Baletemys kampalili (2)	*Limnomys bryophilus* (4)	*Limnomys sibuanus* (5)	*Rattus everetti* (20)	*Tarsomys apoensis* (3)	*Tarsomys echinatus* (1)	*Tarsomys* sp. (1)
TOT	238	293.5 ± 8.39	275.2 ± 9.15	477.61 ± 24.24	270.67 ± 17.01	277	231
	233–243	285–305	266–289	445–523 (18)	258–290		
LT	101	167 ± 4.55	155 ± 9.67	237.06 ± 12.09	129.00 ± 6.24	139	104
	100–102	163–173	147–167	212–260 (18)	124–136		
LHF	31	32 ± 1.41	28.6 ± 0.89	47.55 ± 2.19	33.00 ± 1.00	31	29
	30–32	31–34	28–30	44–53	32–34		
EAR	20	21.5 ± 0.58	20.8 ± 0.45	26.11 ± 1.68	22.00 ± 1.73	20	19
	20–20	21–22	20–21	23–29 (18)	21–24		
WT	70.5	57.25 ± 4.72	49.2 ± 7.66	330.65 ± 69.14	86.67 ± 15.89	93	69
	70–71	54–64	39–60	220–490	77–105		
HBL	137	126.5 ± 4.65	120.2 ± 4.38	239.45 ± 20.94	141.67 ± 10.79	138	127
	131–143	121–132	114–126	210–298	134–154		
LT/	0.74	1.32 ± 0.04	1.29 ± 0.11	0.99 ± 0.09	0.91 ± 0.02	1.01	0.82
HBL	0.70–0.78	1.27–1.36	1.18–1.44	0.71–1.09 (18)	0.88–0.93		
LHF/	0.23	0.25 ± 0.01	0.24 ± 0.01	0.20 ± 0.01	0.23 ± 0.01	0.22	0.23
HBL	0.21–0.24	0.24–0.27	0.22–0.25	0.17–0.22	0.22–0.25		
LOF	19	NA	19.5 ± 0.71	29 ± 2.52	13 ± 0	NA	16
	18–20		19–20 (2)	27–32 (3)	13–13 (2)		
TSR	20.5	NA	15.5 ± 2.12	9 ± 1	15 ± 1.41	NA	16
	20–21		14–17 (2)	8–10 (3)	14–16 (2)		

with particular respect to its mammals, were instrumental in characterizing the Philippines as an exceptionally rich center of endemic mammalian diversity, as well as providing exemplary leadership in mentoring of young colleagues and in promoting conservation of the fauna.

Diagnosis.—Phylogenetically defined as a member of the endemic Philippine *Tarsomys* clade of Tribe Rattini in family Muridae (Figs. 3 and 4), distinguished by the following combination of traits: Intermediate in size, ca. 70 g in weight and 135 mm head and body length (Table 2); shrew-like in appearance (Fig. 2), with soft, dense fur, small eyes and ears, and a conical head with a narrow snout; pelage dark russet brown dorsally with moderately sparse guard hairs, and dark grayish ochre ventrally; mystacial vibrissae long, up to ca. 50 mm, reaching beyond tip of ear; two pairs of inguinal mammae; tail proportionally short (74% of HBL), ca. 100 mm, unicolor, and densely covered in dark umber (almost black) hairs both dorsally and ventrally that partially obscure the scales on the tail; claws on manus unusually robust and long, with a nail-like claw on the hallux. Skull (Fig. 7) slender and elongate;

Fig. 7.—Dorsal, ventral, and lateral views of *Baletemys kampalili* FMNH 208788. Approximately times 2.5 magnification.

incisors slightly opisthodont, nongrooved, and narrow (0.84–0.94 mm wide and 2.00–2.08 mm deep); rostrum long, narrow, and tapering; zygomatic plate narrow, about twice the width of zygomatic arches; orbitotemporal opening proportionally small, with zygomatic arches short and slightly thinner than in other comparably sized Philippine murids, ca. 0.60–0.70 mm at narrowest point (Table 3); descending (anterior) portion of zygomatic arch at shallow angle with respect to dorsal surface of skull, and with lowest extent terminating above the palate. Braincase long and narrow anteriorly but widening posteriorly, smooth and ellipsoidal, without prominent temporal ridges, supraoccipital ridge nearly absent; maximum width of braincase nearly as wide as zygomatic arches; carotid artery with stapedial and internal branches, the former feeding laterally into the otic capsule through a stapedial foramen, and the latter entering the auditory bulla through a foramen adjacent to the basioccipital shelf (see Fig. 56D in Musser and Heaney 1992); auditory bullae weakly inflated compared to its relatives; pterygoid fossa shallow, nearly flush with the plate formed by the basisphenoid and basioccipital bones; medial lacerate and postglenoid foramina continuous or nearly so; incisive foramina short and narrow, terminating 0.65–1.25 mm anterior to molar rows; posterior margin of bony palate extending slightly beyond posterior margins of third molars. Labial cusp t3 elongated into lamina that is mostly continuous with t2 (Fig. 8); labial cusp t3 on M2 tiny but present; lingual cusp t7 and posterior cingulum absent from all upper molars; posterior labial cusplet on m1 and m2 absent. Mandible slender, with angular and condyloid processes approximately equal in length (Fig. 7).

Morphological description.—Same as for type species, described below.

Baletemys kampalili, new species

Figs. 2, 6, and 7 and Tables 1 and 2

Holotype.—FMNH 208788, a fully adult female collected by Danilo S. Balete on 2 March 2010, field number D. S. Balete 6977. The specimen was initially fixed in formalin and is now stored in 70% ethanol with the skull extracted and cleaned. The skull is in good condition apart from a break in the left zygomatic arch. A muscle tissue sample was taken from the thigh when the specimen was collected, stored in 90% ethanol, and frozen at FMNH. The holotype is currently housed at the FMNH but the skull and fluid-preserved body will be transferred to the National Museum of the Philippines; both paratype specimens and all tissue samples will remain at FMNH.

Type locality.—Primary lower montane forest, 1.75 km south and 4.25 km east of Mt. Kampalili peak, elevation 1,640 m (7.29522°N, 126.31602°E), in Davao Oriental Province, Municipality of Manay, Barangay Taocanga, Sitio Limentuog, Mindanao Island (Fig. 1).

Paratypes.—Two additional specimens were obtained, one each on 23 and 26 May 2007 in upper montane (mossy) forest, 2 km south, 2 km west of Mt. Kampalili peak, elevation 1,900 m (7.28658°N, 126.27525°E), in Davao de Oro Province, Maragusan Municipality, Barangay Langgawisan, Sitio Calluyah (FMNH 194802 and 194804). Of these, FMNH 194802 (D. B. Tablada 1) is a juvenile male, with skull not removed, fixed with formalin and preserved in 70% ethanol, and FMNH 194804 (D. B. Tablada 10) is a young adult male, with skull extracted and in good condition apart from broken pterygoid processes, and the remainder preserved in 70% ethanol. Both specimens had a muscle tissue sample taken from the thigh and preserved in 90% ethanol.

Etymology.—This species is named for Mt. Kampalili, where all specimens have been obtained. The specific epithet is used as a noun in apposition. We suggest "Kampalili shrew-mouse" or "Kampalili baletemys" as the English common name.

Table 3.—List of cranial measurements for *Tarsomys*-clade rodents, including the new genus and species, given in the form mean ± 1 *SD* followed by ranges. Numbers in parentheses indicate the number of individuals sampled for that measurement if less than the *n* for each species given in the column heading.

	Baletemys kampalili (2)	*Limnomys bryophilus* (4)	*Limnomys sibuanus* (4)	*Rattus everetti* (17)	*Tarsomys apoensis* (4)	*Tarsomys echinatus* (1)	*Tarsomys* sp. (1)
BOL	31.22	29.29 ± 0.79	27.73 ± 1.10	47.63 ± 2.20	33.51 ± 1.64	30.51	31.02
	31.08–31.35	28.37–30.01	26.18–28.71	43.11–52.98 (15)	32.17–35.8		
IB	6.21	4.97 ± 0.15	5.12 ± 0.14	7.59 ± 0.29	6.12 ± 0.06	6.46	6.25
	6.18–6.24	4.77–5.05	4.98–5.30	6.91–7.90 (16)	6.07–6.19		
ZB	15.88	17.32 ± 0.26	16.17 ± 0.45	25.81 ± 1.34	17.94 (1)	16.41	17.74
	15.26–16.5	17.03–17.62	15.79–16.8	22.82–28.81 (16)			
MB	13.02	12.39 ± 0.12	12.51 ± 0.19	16.74 ± 0.64	13.79 ± 0.54	13.25	13.03
	12.9–13.13	12.25–12.74	12.24–12.65	15.78–18.29 (16)	13.03–14.32		
LN	13.19	12.29 ± 0.37	11.64 ± 0.70	20.11 ± 1.78	14.95 ± 1.64	13.20	13.91
	12.56–13.82	11.86–12.77	11.03–12.57	16.77–24.30 (16)	13.46–17.10		
LIF	5.13	6.07 ± 0.26	5.64 ± 0.12	9.56 ± 0.72	7.55 ± 0.61	5.87	5.96
	4.99–5.27	5.91–6.45	5.49–5.77	8.04–10.62	6.98–8.39		
DR	6.47	6.47 ± 0.29	6.64 ± 0.26	11.13 ± 0.68	7.45 ± 0.29	7.61	7.26
	6.05–6.89	6.05–6.65	6.44–7.02	10.06–12.73	7.04–7.72		
LR	15.02	12.98 ± 0.46	11.46 ± 0.29	20.40 ± 1.08	15.65 ± 1.18	13.55	14.94
	14.87–15.16	12.57–13.45	11.24–11.88	18.62–23.48 (16)	14.54–17.19		
OL	10.86	12.29 ± 0.36	11.46 ± 0.35	18.38 ± 0.90	12.53 ± 0.80	11.75	12.14
	10.69–11.03	11.94–12.79	10.95–11.76	16.41–20.83 (16)	11.87–13.64		
LM1–3	5.69	5.98 ± 0.18	4.76 ± 0.11	9.67 ± 0.49	6.55 ± 0.45	6.38	6.05
	5.51–5.87	5.79–6.16	4.69–4.93	8.80–10.54	5.88–6.89		
PBM1	6.90	6.87 ± 0.10	6.20 ± 0.17	9.91 ± 0.50	8.40 ± 0.57	7.82	8.03
	6.72–7.07	6.76–6.98	6.08–6.45	9.05–10.67	7.89–9.2		
LD	9.98	8.87 ± 0.36	8.42 ± 0.37	14.46 ± 1.08	10.67 ± 0.89	9.23	9.93
	9.97–9.98	8.51–9.2	7.92–8.79	12.34–17.00	10.06–11.99		
PPL	12.29	12.28 ± 0.42	11.69 ± 0.57	17.58 ± 0.88	11.87 ± 1.04	11.37	11.08
	11.83–12.75	11.86–12.87	10.93–12.26	15.99–19.52 (15)	10.35–12.71		
PBM3	4.15	3.97 ± 0.12	3.83 ± 0.27	6.12 ± 0.63	5.42 ± 0.46	4.30	4.42
	4.07–4.23	3.81–4.08	3.44–4.05	5.00–7.20	4.96–6.04		
HBC	10.60	10.72 ± 0.19	10.62 ± 0.40	14.22 ± 0.62	10.98 ± 0.22	11.58	10.98
	10.37–10.82	10.49–10.92	10.06–11.01	13.47–15.63 (15)	10.69–11.29		
BM1	1.79	1.88 ± 0.02	1.54 ± 0.05	2.74 ± 0.20	1.92 ± 0.05	1.98	1.96
	1.77–1.80	1.85–1.90	1.51–1.62	2.31–3.09	1.87–1.99		
BIT	1.75	1.97 ± 0.09	1.84 ± 0.13	3.35 ± 0.26	2.04 ± 0.18	1.90	1.93
	1.64–1.86	1.88–2.08	1.69–2.00	2.83–3.97	1.87–2.21		
BZP	2.65	2.87 ± 0.07	2.77 ± 0.07	6.03 ± 0.50	4.11 ± 0.19	3.56	4.12
	2.53–2.76	2.79–2.93	2.71–2.86	4.74–6.77	3.92–4.29		
BOL/ZB	1.97	1.69 ± 0.04	1.72 ± 0.07	1.85 ± 0.04	1.81 (1)	1.86	1.75
	1.90–2.04	1.66–1.74	1.62–1.77	1.78–1.93(15)			
OL/BOL	0.348	0.419 ± 0.01	0.413 ± 0.01	0.386 ± 0.01	0.374 ± 0.01	0.385	0.391
	0.344–0.352	0.412–0.428	0.408–0.418	0.364–0.412 (15)	0.365–0.381		
LR/BOL	0.481	0.443 ± 0.01	0.414 ± 0.01	0.428 ± 0.01	0.466 ± 0.01	0.444	0.482
	0.478–0.484	0.435–0.450	0.402–0.434	0.385–0.448 (14)	0.452–0.480		

Geographic distribution.—Known only from two localities, about 6 km apart, on the southern slopes of Mt. Kampalili, but probably widely distributed above 1,450 m on the peaks surrounding Mt. Kampalili (Fig. 1).

Diagnosis.—Because *Baletemys kampalili* is the only known species of *Baletemys*, generic and specific diagnoses are the same.

Morphological description and comparisons.—A stocky animal with a head that is small relative to body size, with an elongated, cone-shaped snout (Fig. 2). *Baletemys kampalili* is slightly smaller (HBL 131–143 mm) than *T. apoensis* (HBL 134–154 mm), substantially smaller than *R. everetti* (HBL 210–298 mm), larger than *L. sibuanus* (HBL 114–126 mm), and similar in body size to *T. echinatus* (HBL 138; Table 2; Fig. 5). *Rattus everetti*, on account of its much larger size, relatively shorter rostrum (LR/BOL 0.428 compared to 0.481), relatively larger eyes (OL/BOL 0.386 compared to 0.348), and relatively longer tail (LT/HBL 0.99 compared to 0.74), is easily distinguishable from *B. kampalili*. Similarly, *Limnomys* is easily distinguishable based on its smaller size, relatively shorter rostrum (LR/BOL 0.414, *L. sibuanus*; 0.443, *L. bryophilus*), relatively wider skull (BOL/ZB 1.72, *L. sibuanus*; 1.69, *L. bryophilus*; compared to 1.97 in *B. kampalili*; Table 3), and much longer tail (LT/HBL 1.29, *L. sibuanus*; 1.32, *L. bryophilus*; Table 2). Although relevant specimens are unavailable for comparison, Musser (1981) described *K. sodyi* as an arboreal rodent with a long tail (longer than head and body length), strong pelage countershading, incisive foramina reaching or extending beyond the anterior edge of the first molar, and molar cusps discrete. As such, most of our detailed comparisons focus on

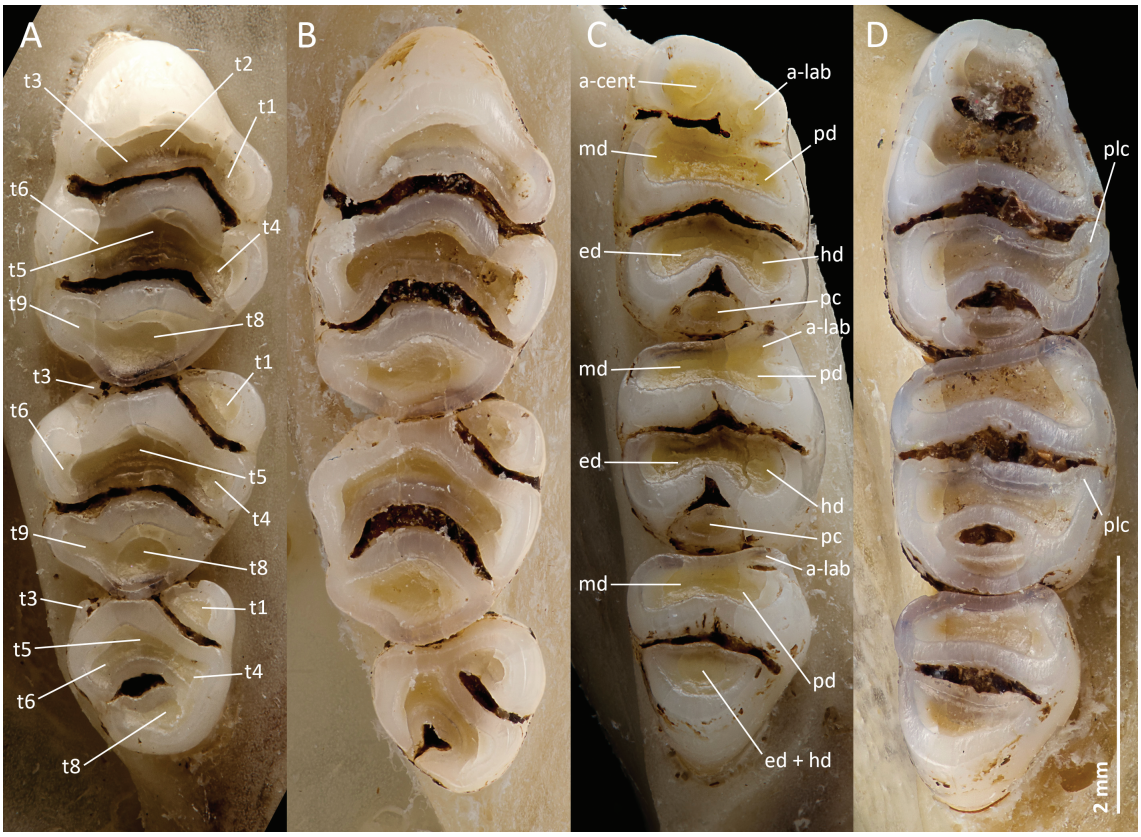

Fig. 8.—Detail of upper (A, B) and lower (C, D) right molar rows for *Baletemys kampalili* FMNH 194804 (A, C) and *Tarsomys apoensis* FMNH 148176 (B, D). Lettering indicates cusps according to notation of Musser and Heaney (1992). a-cent: anterocentral cusp; a-lab: anterolabial cusp; md: metaconid; pd: paraconid; ed: entoconid; hd: hypoconid; pc: posterior cingulum; plc: posterior labial cusplet.

distinguishing *Tarsomys* from *B. kampalili*, with some comparisons with *R. everetti* and *L. sibuanus*. Where necessary, we make additional comparisons with *K. sodyi* based on the description by Musser (1981).

The head shape of *B. kampalili* is perhaps the most distinctive feature of the species compared to its close relatives: it is long, narrow, and roughly conical. *Limnomys sibuanus*, *R. everetti*, all *Tarsomys* species, and *K. sodyi* instead have stout, broad heads that more closely resemble a generalized rat. The ears are short, but longer than wide: on the holotype, these are 13.5 mm wide and 20 mm long, with tips that are broad and rounded. The ears are comparably sized in *T. echinatus* (EAR: 20 mm) and *T.* sp. from Mt. Kampalili (EAR: 19 mm) but slightly larger in *T. apoensis* (EAR: 22 mm), in which specimens had ears up to 24 mm long. Both sides of the pinna are covered in very fine, short hairs throughout. These hairs are smoky red-brown at the base of the ears and progressively darken to dark umber at the tips.

The tail is short, about 77% of head and body length in the holotype, 70% in FMNH 194804 (Table 2), and 77% in FMNH 194802, a juvenile, which is proportionally shorter than any other species in the *Tarsomys* clade (maximum LT/HBL, 132%, *L. bryophilus*; minimum 82%, *Tarsomys* sp.; Table 2). The tail has short, fine hairs projecting from underneath the posterior margin of each scale, three per scale. These hairs gradually increase in length from the base to the tip of the tail, partially obscuring the scales. The hairs form a small tuft extending approximately 0.5 mm beyond the end of the tail. The tail is more densely haired than any other species in the *Tarsomys* clade.

Overall, the pelage of *B. kampalili* is soft, dense, and relatively uniform in its density, with three hair types in two layers. The pelage color is russet brown dorsally, transitioning gradually along the ventrolateral margin to grayish ochre on the ventral surface. The overfur consists of black guard hairs that are moderate in density but decrease in length and number anteriorly. These hairs project as much as 2–5 mm above the underfur along the mid-dorsum. Guard hairs are much less common relative to the dense, soft underfur in *B. kampalili* compared to other *Tarsomys*-clade species, particularly in *T. echinatus*, which exhibits a layer of spiny awn hairs not found in any other member of the *Tarsomys* clade. All fur exhibits a short ashen-gray portion from the base to approximately 2 mm from the skin. The layer of underfur contains two hair types: golden-tipped awn hairs, which are very dense within the dorsal pelage but become less abundant ventrally, and underhairs that are almost entirely ashen gray, denser on the ventral surface, thinner, and shorter than awns. With the exception of *T. apoensis*, which has more yellowish fur ventrally, other members of the *Tarsomys* clade have pale, grayish ventral fur (i.e., prominent countershading). Additionally, *Limnomys* and *R. everetti* lack the dark

brown dorsal fur that characterizes *B. kampalili*; *L. sibuanus* is burnt orange dorsally and yellowish cream ventrally, whereas *R. everetti* ranges from medium gray to gray-brown dorsally that transitions to dark brown toward the mid-dorsum, and ventrally to a cream or sandy gray. The pelage of *T. apoensis* is brighter and more orange-red compared to *B. kampalili*, which is a dark cinnamon color dorsally and pale mustard ventrally. *Kadarsanomys sodyi* exhibits dark brown pelage dorsally that fades to gray laterally and additionally exhibits strong countershading, with white underparts (Musser 1981).

Overall, the head is entirely furred, with only the nares completely lacking hairs; even the dorsal surface of the rhinarium and lips are covered by short, fine hairs. The upper lip adjacent to the philtrum is haired but the interior surfaces are naked. The lower lip is finely haired. The pigmentation of the hairs shifts from smoky red-brown near the back of the head to unpigmented along the lateral and anterior margins of the snout. The mouth is small, and both upper and lower incisors are visible when the mouth is closed. Mystacial vibrissae protrude along the lateral surface of the rostrum between approximately one-fifth and three-fourths of the distance between the tip of the rostrum and the anterior margin of the eye, up to 47 mm long, dark brown at base and fading to unpigmented near tip, reaching well beyond the base of the ears. The dorsal margin of vibrissae emergence occurs along a line that runs from the naris to the eye. Anteroventrally, the vibrissae occur along a margin that ends about two-thirds the distance from the dorsum of the rostrum to the upper lip. Three long (8–10 mm) inter-ramal vibrissae project below the mandibular joint. Submental vibrissae on the lower lip are up to 5 mm long and unpigmented.

The eye openings of *Baletemys* are small, ca. 3.5–4 mm, relatively smaller than other species in this clade. A band of naked skin, ca. 0.5 mm wide, subtends the lower edge of the eye opening. The upper edge has fine eyelashes, ca. 1.5 mm long. There are two supraciliary vibrissae, 22–24 mm long, and one or two genal vibrissae, ca. 20 mm long.

The forefeet are relatively small, pigmented pale brown dorsally and ventrally, and have large, deep, robust claws that are darkly pigmented. On digits 2–4 the foreclaws are slightly curved and notably long, approximately the length of the first phalanx. *Baletemys kampalili* has proportionally, notably longer claws on the manus compared to *L. sibuanus*, *R. everetti*, and *T. apoensis*. The claw lengths of the pes are slightly longer in *T. apoensis* and *L. sibuanus*, and similar in *R. everetti*.

Digit 1 (the hallux) is very small, nearly fused to the medial face of the manus, and has a square nail-like claw. Digits 2 through 5 exhibit rings of scales along each individual digit. Digits 3 and 4 are approximately equal in length, whereas 2 is shorter and 5 is shortest. The dorsal surface of the manus exhibits fine (dark umber) hairs that become unpigmented/white toward the digits. Five to six unpigmented antebrachial vibrissae, ca. 5–8 mm long, are on the lateral margin at the base of the wrist. The plantar pads of the manus are large, angular, and highly raised from the surface, with the thenar and hypothenar being rectangular and interdigital pads triangular. The vertices of the interdigital pads roughly converge on a point at the center of the manus and occupy most of the surface of the manus.

The pes, including its claws and digits, is dark brown dorsally and ventrally, and is relatively long (30–32 mm) and narrow (ca. 5–6 mm), and between 21% and 24% the length of the head and body (Table 2). The digits constitute approximately three-eighths of this length and exhibit robust claws, although these are shorter than those of the manus. Digit 1 (the pollex) is shorter than the remaining four digits, which are of approximately equal length. The dorsal surface of the pes is finely haired with umber hairs that extend to the tips of the digits. The interdigital pads of the pes are less angular than those of the manus but large and roughly triangular in shape, converging on a point in the center of the pes. The hypothenar is elongate and reniform, whereas the thenar is slightly ellipsoidal.

The holotype, an adult female, exhibits two pairs of inguinal mammae, compared to the three pairs (two inguinal and one axillary) exhibited by *Limnomys* and *Tarsomys* and four pairs exhibited by *R. everetti* and *K. sodyi* (Musser and Heaney 1992; Heaney et al. 2016b); in this respect, *Baletemys* resembles species of Phloeomyini and Chrotomyini, all of which have two pairs of inguinal mammae (Heaney et al. 2016b). The urinary papilla is ca. 8 mm long and 4 mm wide, has unpigmented skin, and is sparsely haired. Scattered hairs on the basal two-thirds of the papilla are dark brown, 1–3 mm long. About 10 sparse, scattered hairs on the distal one-third are unpigmented, 5–11 mm long, projecting well beyond the tip of the papilla, forming a poorly defined tuft.

The penis sheath on FMNH 194804, a young adult male, is ca. 9 mm long and 5 mm wide; the skin is unpigmented. Sparse, scattered hairs on the basal two-thirds of the sheath are dark brown, 1–3 mm long. About 12 unpigmented hairs on the distal one-third of the sheath are 8–15 mm long, projecting well beyond the tip of the sheath, forming a poorly defined tuft. The scrotum is large and conspicuous, ca. 30 mm long and 15 mm wide, extending from the base of the penis sheath to the anus. With the exception of the posterior tip, the skin is unpigmented but entirely covered by short, dark brown hairs that are sparser ventrally and denser and longer laterally and dorsally. The posterior tip has an area ca. 5 × 5 mm that lacks hairs and is pigmented dark brown.

The skull is long and narrow (BOL/ZB 1.97; Fig. 7), proportionally more so than all other members of the *Tarsomys* clade (maximum BOL/ZB 1.86 in *T. echinatus*; minimum BOL/ZB 1.69 in *L. bryophilus*; Table 3). The rostrum is long and narrow (LR/BOL 0.481; Table 3), and tapers anteriorly. The nasals are roughly teardrop-shaped, widest near their anterior margin, and narrow progressively toward the braincase, where the bone becomes thinner and almost translucent. The anterior edge of the nasals projects beyond the incisors. The premaxillary terminates laterally alongside the nasals, and the incisor root, which is visible through the translucent premaxillary, terminates along the curved lateral suture between the premaxillary and maxillary bones.

There is a small wing-like process of the lacrimal that attaches to the maxillary and frontal bones that juts laterally

from the dorsal surface of the skull. The zygomatic spine formed by the anterodorsal margin of the zygomatic plate is slight, exhibiting only a gentle shoulder. Otherwise, this spine gradually slopes to the posterolateral edge of the rostrum. The zygomatic plate is narrow, about twice the width of the zygomatic arch at the widest point of the plate. The posterior margin of the zygomatic plate is oriented almost vertically, but the anterior margin slopes anteroventrally/posterodorsally, making the plate roughly triangular in shape from the lateral and ventral aspects (Fig. 7). The squamosal process of the zygomatic arch terminates more ventrally along the skull than the maxillary process of the zygomatic arch, attaching to an 8.1 mm long horizontal ridge about five times the width of the arch itself that forms a shelf along the squamosal bone. The angle of the descending (anterior) portion of the zygomatic arch is noticeably shallow, terminating well above the ventral surface of the skull at the base of the molars when viewed laterally.

The branching of the zygomatic arch to form the infraorbital foramen is easily visible from the dorsal and lateral aspects of the skull. The infraorbital foramina are large and roughly teardrop-shaped in anterior view. In both the holotype and paratype (FMNH 194804), the nasolacrimal capsule expands slightly inside the infraorbital foramen, partially obstructing the foramen. In paratype FMNH 194804, the infraorbital foramen opens into a lateral fissure anterior to the foramen.

The orbit is small, consistent with the small eyes of the species, and proportionally the smallest in the *Tarsomys* clade (Table 3). The interorbital region is hourglass-shaped. Each frontal bone is inflated dorsally and laterally in a chambered fashion. The top and sides of the frontal bone have net-like patterns that web across these inflated portions in the paratype, but the holotype lacks this netting. The zygomatic arch is less concave dorsoventrally than most other *Tarsomys*-clade species; this is largely due to the shallower angle at which the zygomatic process of the maxillary projects relative to the plane of the skull, which is larger in all other species of the *Tarsomys* clade besides *L. bryophilus* (Fig. 6; Figs. 22 and 77 in Musser and Heaney 1992; Fig. 5 in Rickart et al. 2003).

The braincase is ellipsoidal and smooth, with barely evident temporal ridges; the supraoccipital ridge is nearly absent, appearing more as a gentle slope than a prominent ridge. In contrast, the braincase is much more angular in other *Tarsomys*-clade species, particularly *R. everetti*, but to a lesser extent *Limnomys* and *T. echinatus*. The bones comprising the braincase are somewhat thin, with the parietals and much of the occipital almost translucent. The interparietal is short and wide but altogether rounded, almost rhomboid in shape but with the anterodorsal vertex having a wider angle than the posterior vertex. The mastoid is inflated and exhibits a prominent exoccipital process.

The occipital condyles (Fig. 7) project ventrally from the basioccipital such that the basicranium appears somewhat excavated. There is substantial variation in the extent of perforation of the basicranial region between the two adult specimens of *B. kampalili*: the holotype exhibits more extensive ossification of the basicranium, including the isthmus between the postglenoid and medial lacerate foramina, the postglenoid foramen on the left side of the skull, and the anterior portion of the sphenopalatine vacuities, which are obscured by a translucent layer of bone. In the paratype, all of these structures are unobstructed. The near confluence of the postglenoid and medial lacerate foramina is a character that distinguishes this rodent from other *Tarsomys*-clade members such as *T. apoensis*, in which the foramina are distinctly separate and separated by opaque bone (Fig. 7; Fig. 17 in Musser and Heaney 1992). Like other *Tarsomys*-clade species, the occipital condyles are not visible in a dorsal view of the skull and are instead obscured by the posterior portion of the braincase.

The sphenopterygoid vacuity is longest along the major axis of the skull and separated from the sphenopalatine vacuity only by thin branches of the pterygoid. The sphenopalatine vacuity does not extend anteriorly to the edge of the hard palate along the basisphenoid. Anteromedially adjacent to the prominent bony eustachian tube, the transverse canal is subdivided below the surface of the basicranium (i.e., visible only when peering into the foramen; Fig. 7). The auditory bullae are moderately inflated. Anteriorly, the bullae are largely separated from the surrounding bone by the medial lacerate and postglenoid foramina. The divisions in the bulla are readily visible due to the prominent septum dividing the two chambers. The asymmetrical division occurs along the lateral-most fourth of the bulla and gives the bulla a somewhat helical shape when viewed laterally. *Baletemys kampalili*, like other members of the *Tarsomys* clade, displays a cephalic arterial pattern that resembles the "primitive" pattern of muroid rodents described by Musser and Heaney (1992, Fig. 56D): the common carotid artery appears to branch into a stapedial and internal branch, the former of which feeds laterally into the otic capsule through a stapedial foramen and the latter of which enters the auditory bulla through a foramen adjacent to the basioccipital shelf.

Anterolateral to the foramen ovale is the shelf formed by the pterygoid plate (Fig. 7). The pterygoid fossa is so shallow as to be almost coplanar with the rest of the occipital shelf. The anterior opening of the alisphenoid canal is divided on the left side of the paratype by a thin dorsoventrally oriented strut but is undivided on the right; the holotype exhibits these struts on both sides of the skull. The division constitutes the septum between the anterior opening of the alisphenoid canal and the foramen ovale. Anterior to the alisphenoid canal is the alar fissure, which is subdivided into two foramina, the anterior lacerate foramen (dorsal) and an extension of the sphenopalatine vacuity (ventral), recessed posteriorly inside the fissure and which open directly into the braincase. The palate is wide and exhibits a prominent groove aligned with each incisive foramen lingual to each molar row (Fig. 7). The molar shelf is relatively deep and clearly delineated, but more gradual than the slope exhibited by *T. apoensis*, *L. sibuanus*, and *R. everetti.*

The upper incisors are slightly opisthodont (unique among all species analyzed in this study; all others have orthodont incisors), rectangular anteriorly, and lack grooves on the anterior surface. Each incisor is 4.68 mm long, 0.92 mm wide, and 2.08 mm deep for the holotype and 5.21 mm long, 0.84 mm

wide, and 2.00 mm deep for FMNH 194804. The molars (Fig. 8A and C) are similar to those of *T. apoensis* (Fig. 8B and D), as described in detail in Musser and Heaney (1992; see their Figs. 11–13), although proportionally smaller in *B. kampalili* relative to the size of the skull (Table 3). The molars in *B. kampalili*, *T. apoensis*, and Mt. Kampalili *Tarsomys* sp. are generally configured as laminae formed by the cusps bracketing deep valleys. The molars of the two adult specimens of *B. kampalili* are too worn to make useful comparisons of molar crown height among species. Fossae between molar laminae are proportionally wider in *L. sibuanus* and *R. everetti* than in *B. kampalili*. Cusps on upper and lower molars are inclined slightly posteriorly, especially the lower molars. The first upper molar is the largest, M2 is two-thirds of its length, and M3 is one-half of its length; in *T. apoensis*, M3 is proportionately slightly smaller, whereas it is proportionately larger in *L. sibuanus* and *R. everetti*. The anterior margin of M1, particularly along the major axis of the tooth, protrudes anteriorly, giving the anterior edge a lambdoid shape in lateral view. Like *T. apoensis*, the lamina between t3 and t2 on M1 is relatively unconstructed, in contrast to *L. sibuanus* and *R. everetti*, where the lamina is pinched, making t3 appear more distinct. Cusp t7 is absent on all molars, and no posterior cingulum is present. This differs from the condition of *L. sibuanus* and *R. everetti*, in which a posterior cingulum is present on M1 and M2 (Figs. 25 and 78 in Musser and Heaney 1992). Labial cusp t3 is present as a tiny mound on M2 and M3 of our two specimens; these are present on about two-thirds and one-half of nine *T. apoensis* for each molar respectively (see Table 4 in Musser and Heaney, 1992). Lower molars of *B. kampalili* are similar to those of *T. apoensis*, though slightly reduced in length and width (Fig. 8). The anterior labial cusp is present on m1 and m2, but the posterior labial cusplet that is usually present on *T. apoensis* (Table 4 in Musser and Heaney 1992) is absent in the two *B. kampalili* sampled.

The mandible of *B. kampalili* is narrow and slender (Fig. 7). The coronoid process is narrow but extensive and curves posteriorly, coming to a point. The condyloid process is set relatively low and projects posteriorly, almost horizontal along the major axis of the mandible, as does the similarly narrow angular process. The mandible edges between the posterior processes are highly concave. The mandibular shelf extends from the anterior margin of the molar row to the apex of the concavity between the coronoid and condyloid processes. The mandibular foramen occurs dorsally almost adjacent to this shelf.

Ecology.—The holotype was captured at 1,640 m elevation in lightly disturbed primary lower montane forest near a stream. It was caught during the daytime in a snap-trap baited with coconut coated in peanut butter that was set along a runway through groundcover plants. Nearby tree species included predominantly oaks (*Lithocarpus*), myrtles (*Syzygium*), laurels (*Litsea*), and elaeocarps (*Elaeocarpus*), with a canopy height of ca. 12–20 m. *Ficus* and *Rhododendron* were common in the understory, with gingers, moss, ferns, and grasses as ground cover. Epiphytes included moss, orchids, ferns, lichens, and small *Rhododendron* and *Medinilla*; canopy vines of *Freycinetia*, *Tetrastigma*, *Smilax*, and *Calamus* were abundant. Leaf litter was abundant, lying above a thick layer of humus. Other small mammals trapped at the type locality in 465 trap-nights were *Crocidura beatus*, *Podogymnura* sp., *Apomys* sp., *Bullimus bagobus*, *R. everetti*, and *Tarsomys* sp. *Cynocephalus volans*, *Paradoxurus philippinensis*, *Sus philippensis*, and *Rusa marianna* were either sighted or left clear evidence of their occurrence.

Paratypes FMNH 194802 and 194804 were collected in mossy forest at 1,900 m, approximately 450 m higher than the holotype. These specimens were captured, respectively, underneath a moss-covered rotten log and beside a moss-covered log on a steep slope, using snap rat traps baited with live earthworms. Shrubs, epiphytes, and rattan were abundant in the surrounding habitat, and the soil at the collection site was loose, with a thick humus layer. The conifer *Dacrycarpus cumingii* was the dominant tree species. Other nonvolant small mammals captured at this locality were *Podogymnura* sp., *Sundasciurus philippinensis*, *Apomys* sp., *B. bagobus*, *R. everetti*, and *Tarsomys* sp. All specimens collected on Mt. Kampalili are currently deposited in FMNH; currently unidentified species are under study to ascertain their distinctiveness.

The elevations at which individuals were captured (1,640 and 1,900 m) lie within the range of old-growth montane and mossy forest (Fernando et al. 2008) in which oaks, conifers, and laurels are common canopy trees, and moss, epiphytes, and ground plants are abundant. These high-elevation forests typically exhibit a deep humus layer that provides habitat for earthworms consumed by many nonvolant mammalian species (Heaney et al. 2016b), likely including *Baletemys* (two of three specimens were captured in traps baited with earthworms). We captured no *B. kampalili* in nearby lowland forest, which originally reached to about 1,100 m but most had been logged and converted to agriculture. During our studies, some areas of disturbed montane forest occurred up to 1,550 m, but the montane and mossy forest where *Baletemys* was captured was relatively undisturbed. No trapping was conducted above 1,900 m, so the upper elevational range of *B. kampalili* is unknown, and may potentially extend to the peak of Mt. Kampalili (~2,396 m).

Discussion

Diversification of the Tarsomys *clade.*—The distribution of *Tarsomys*-clade individuals in component space (Fig. 5) suggests that size and shape of the cranium are highly correlated. Each genus in this clade is morphologically distinct in terms of both size and shape, from the small, long-tailed, soft-furred *Limnomys* to the much larger, harsh-furred *R. everetti* which more closely resembles species such as *R. norvegicus* or *R. tanezumi* in some respects (see our discussion on the taxonomy of *Rattus* below). Intermediate between these two genera are *T. apoensis*, Mt. Kampalili *Tarsomys* sp., and *B. kampalili*, which each resemble shrew-mice though to different degrees, including the shape of the skull, short tail, robustness of the claws, and dark pelage with limited countershading. Given the recent radiation of the *Tarsomys* clade (the crown age of which

is less than 2.5 million years old; Fig. 4), the patterns we see within this clade seem to mimic, on a small scale, the diversity of other island-endemic groups in the Indo-Australian archipelago, including Chrotomyini of the Philippines, Hydromyini of Sahul, and *Maxomys*/*Crunomys* of Wallacea (sensu Ali and Heaney 2021), in that the species in these clades vary substantially in their ecology based on available natural history information (Heaney et al. 2006, 2016b; Rowe et al. 2016). Although available relevant ecological information for *B. kampalili* precludes anything but inferences, the addition of the *Tarsomys* clade to the growing list of archipelago-endemic murine lineages with morphologically distinct species or genera suggests that ecomorphological diversification may have happened rapidly and consistently across several different Indo-Australian rodent radiations without major shifts in evolutionary tempo or mode among these major clades (Alhajeri et al. 2016; Rowsey et al. 2019; Marcy et al. 2020). Further research on this topic examining morphological evolution among major lineages in the Indo-Australian archipelago clearly is warranted.

Taxonomy of Rattus *and the* Tarsomys *clade.*—Our decision to describe *B. kampalili* as a new genus and species warrants comment in two respects. First, our results, like several prior studies (e.g., Rowe et al. 2011, 2019; Schenk et al. 2013) illustrate the polyphyly of *Rattus* as currently defined, with four major lineages: (i) a widespread clade found in mainland Eurasia and the Sunda shelf and Wallacea (*Rattus* sensu stricto), (ii) a clade endemic to Sahul and Wallacea, (iii) *R. timorensis* in a clade with taxa endemic to lesser Sunda (Rowe et al. 2019), and (iv) *R. everetti*. While no phylogenetic inference so far has been able to definitively establish the monophyly of each of these four clades containing *Rattus* species, this pattern is nevertheless consistent across studies, which have built on an existing multilocus data set with increasing taxon sampling and analyzed using different methods. Uniting all these *Rattus* lineages would involve subsuming at least 16 genera of murines in the tribe Rattini, including *Bandicota*, *Bullimus*, *Bunomys*, *Diplothrix*, *Eropeplus*, *Frateromys*, *Halmaheramys*, *Kadarsanomys*, *Komodomys*, *Lenomys, Limnomys*, *Paruromys*, *Papagomys*, *Sundamys*, *Taeromys*, and *Tarsomys*. Furthermore, the position of *R. everetti*, a species endemic to the oceanic Philippines and nested within a clade of highly distinct species in different genera, suggests that subsuming the genera in the *Tarsomys* clade into the genus *Rattus* would obscure more than it elucidates. We advocate, given additional phylogenetic coverage, a redefinition of *Rattus* to include only the *Rattus* sensu stricto clade, with new names assigned to Sahulian *Rattus* and their relatives in Wallacea, to *R. timorensis*, and to *R. everetti* and the animal referred to here as the "Sibuyan rat" (Figs. 3 and 4).

Similarly, one might suggest that the genus *Tarsomys* could be redefined to include all members of what we here call the *Tarsomys* clade. We note that each of the genera we recognize here, plus the inferred eventual recognition of the *R. everetti* group as a distinct genus, is morphologically distinct and genetically definable, as shown above. Further, each is ecologically distinct: *Tarsomys* are ground-living species that feed mostly on a range of invertebrates but also some plant material; *Limnomys* are more omnivorous and may be largely arboreal; *Baletemys* is likely a specialist that principally feeds on earthworms and other soft-bodied invertebrates; and *R. everetti* is a quite large, highly omnivorous rat that forages on the ground and in trees (Heaney et al. 2006 and data presented here). Including such diverse taxa in a single genus would run contrary to current trends in mammalian taxonomy, and would obscure important differences.

Biogeographic and conservation implications.—At ca. 98,000 km^2, Mindanao is the second largest island in the Philippines, and one of the largest oceanic islands in the world. Studies of its mammalian fauna began in the middle to late 1800s, but were limited in scope and were predominantly conducted in the lowlands, where most species tend to be widespread (Elera 1915; Taylor 1934). From about 1900 to the early 1950s, field work became more intensive and often extended into mountainous terrain in central Mindanao (e.g., Mearns 1905; Hollister 1913; Dickerson et al. 1928; Hoogstraal 1951; Sanborn 1952, 1953), where locally endemic mammalian species were discovered. Subsequent field and museum studies documented several more locally endemic species (Rabor 1966; Musser 1982a, 1982b; Musser and Heaney 1992; Musser et al. 1998; Rickart et al. 2003), but most of these came from the same set of mountains as the earlier studies, especially Mt. Apo and Mt. Kitanglad in central Mindanao (Fig. 1). This led to a view of the Mindanao fauna of nonvolant mammals as containing many widespread lowland species and a relatively small number of locally endemic species from just a few mountains in central Mindanao (e.g., Heaney 1986, 2004; Heaney et al. 1998, 2006). This perspective has begun to change due to field surveys in eastern Mindanao after 2000, leading initially to the description of *Batomys hamiguitan* Balete et al. 2008 (see also Balete et al. 2006) from Mt. Hamiguitan in the far southeastern peninsula of Mindanao, and now to *Baletemys kampalili* from Mt. Kampalili in southeastern Mindanao (Fig. 1).

In retrospect, the recent discovery of these previously unknown, locally endemic small mammals at high elevation on isolated mountain ranges should come as no surprise. Studies of small mammals on Luzon, in the northern Philippines, with a similar number of isolated mountain ranges, have resulted in the discovery of ca. 28 species of locally endemic montane mammals since 2000, doubling the number of native nonvolant mammals on Luzon from 28 to ca. 56 (Heaney et al. 2016a, 2016b; Rickart et al. 2019). We predict that continuing study of small mammals on the many isolated mountains of Mindanao will yield many additional new species. Indeed, based on results from Luzon, we project that every isolated mountain range on Mindanao will be found to support a unique set of endemic mammals. In this regard, we make two specific predictions: first, that the mountains of eastern Mindanao will produce far more locally endemic mammals than the two (*Baletemys kampalili* and *Batomys hamiguitan*) currently known. The presence on Mt. Kampalili of the endemic *Rafflesia verrucosa* (a parasitic "corpse flower") is an indication that this area may be a generally important center of biological endemism on Mindanao

(Balete et al. 2010), as well as a key area for conservation of the endangered Philippine Eagle (Mallari et al. 2001). The presence of three potentially distinct species of small mammals currently under study (*Podogymnura* sp., *Apomys* sp., *Tarsomys* sp.) may corroborate this prediction. Second, we predict that isolated "sky islands" such as Mt. Hilong-Hilong in northeastern Mindanao and Mts. Busa, Daguma, and Matutum in southwestern Mindanao (Fig. 1) will produce additional locally endemic species. If our predictions are accurate, the new species discovered in these areas will contribute significantly to the continuing rise in mammalian species recognized globally (Burgin et al. 2018; Moura and Jetz 2021).

As reported by Balete et al. (2010), the tropical montane forest of the Philippines is under threat from fragmentation and disturbance, with Mt. Kampalili especially impacted by clearing for abaca plantations, extending at least to 1,100 m elevation. A 2002 analysis of satellite imagery conducted by Environmental Science for Social Change, in conjunction with the Philippine Tropical Forest Fund and The Philippines Department of Environment and Natural Resources, illustrates that Davao de Oro and Davao Oriental Provinces, the provinces that include Mt. Kampalili, only contain roughly 40% forest cover over areas greater than 100 m elevation and with a slope steeper than 18° (Walpole 2010). The Mts. Puting Bato–Kampalili–Mayo complex as a whole has been historically impacted by clear-cut logging facilitated by large-scale road construction beginning in the 1950s that continue to allow mining activities and logging, particularly at low and mid-elevation forest (Kummer 1992; Mallari et al. 2001). We thus reiterate the previous recommendations of Balete et al. (2010) calling for protection of the Mt. Kampalili range in collaboration with local communities to ensure the continued existence of the watersheds on which human populations depend, along with *B. kampalili* and other species that may be confined to the montane forests of Mt. Kampalili.

Acknowledgments

D. Salvador and staff of the Philippine Eagle Foundation provided logistical support and administrative assistance that made the fieldwork on Mt. Kampalili possible. The field team was led by D. S. Balete, and assisted by J. Sarmiento, R. Quidlat, M. Silvosa, and D. Tablada. We are thankful for the hospitality of the local residents of barangays Langgawisan and Taocanga, and for their assistance as cooks, guides, and porters. Permission to conduct fieldwork was granted by the Department of Environment and Natural Resources (DENR)—Region XI, with the cooperation of the local government units of Maragusan and Manay Municipalities. Funding for field work was provided by the Critical Ecosystem Partnership Fund, through the Eastern Mindanao Corridor project of the Philippine Eagle Foundation Inc. and Conservation International (CI). Funding for museum studies was provided by the Barbara Brown Fund for Mammal Research of the Field Museum, the Negaunee Foundation, and the Grainger Foundation. DMR was funded by a Barbara Brown Postdoctoral Fellowship. We thank A. Ferguson, J. Phelps, and L. Johnson for assistance with voucher specimens and tissues used in this study; L. Nassef for generating skull photographs; V. Simeonovski for the drawing of *Baletemys kampalili*; K. Feldheim and I. Distefano for laboratory assistance; and C. Kyriazis for generating some of the molecular sequence data used in this study. We thank the Collaborative Invertebrate Laboratories at FMNH and Drs. Petra Sierwald and Rüdiger Bieler for use of imaging equipment (funded by the National Science Foundation). We also thank Stephanie Ware, Manager of Morphology Labs at FMNH for equipment training and support. We take special pleasure in naming this new genus in honor of Danilo S. Balete, in recognition of his lifelong contributions to understanding, conserving, and enjoying the outstanding biodiversity of the Philippines.

Supplementary Data

Supplementary data are available at *Journal of Mammalogy* online.

Supplementary Data SD1.—GenBank accession numbers for sequences used in this study.

Supplementary Data SD2.—PCR protocols and primers used for DNA sequence amplification.

Supplementary Data SD3.—Alignment of sequences used in this study in Nexus file format.

Supplementary Data SD4.—PartitionFinder best-fit nucleotide substitution model partitioning schemes for phylogenetic analyses.

Supplementary Data SD5.—Maximum likelihood phylogenetic tree generated from multilocus concatenated nuclear sequence data. Branch lengths are proportional to number of nucleotide substitutions. Dots at nodes indicate bootstrap support. Individuals within species with strong nodal support have been collapsed when three or more individuals have been sampled, with the number sampled in parentheses after the species name.

Supplementary Data SD6.—Raw measurements and metadata of specimens included in the study.

Literature Cited

Achmadi A.S., Esselstyn J.A., Rowe K.C., Maryanto I., Abdullah M.T. 2013. Phylogeny, diversity, and biogeography of Southeast Asian spiny rats (*Maxomys*). Journal of Mammalogy 94:1412–1423.

Aghová T., Kimura Y., Bryja J., Dobigny G., Granjon L., Kergoat G.J. 2018. Fossils know it best: using a new set of fossil calibrations to improve the temporal phylogenetic framework of murid rodents (Rodentia: Muridae). Molecular Phylogenetics and Evolution 128:98–111.

Alhajeri B.H., Schenk J.J., Steppan S.J. 2016. Ecomorphological diversification following continental colonization in muroid rodents (Rodentia: Muroidea). Biological Journal of the Linnean Society 117:463–481.

Ali J.R., Heaney L.R. 2021. Wallace's line, Wallacea, and associated divides and areas: history of a tortuous tangle of ideas and labels. Biological Reviews 96:922–942.

Balete D.S., Heaney L.R., Rickart E.A., Quidlat R.S., Ibañez J.C. 2008. A new species of *Batomys* (Mammalia: Muridae)

from eastern Mindanao Island, Philippines. Proceedings of the Biological Society of Washington 121:411–428.

Balete D.S., Pelser P.B., Nickrent D.L., Barcelona J.F. 2010. *Rafflesia verrucosa* (Rafflesiaceae), a new species of small-flowered *Rafflesia* from eastern Mindanao, Philippines. Phytotaxa 10:49–57.

Balete D.S., Quidlat R.S., Ibañez J.C. 2006. Non-volant mammals of Mt. Hamiguitan, eastern Mindanao, Philippines. Banwa 3:65–80.

Balete D.S., Rickart E.A., Heaney L.R., Alviola P.A., Duya M.V., Duya M.R.M., Sosa T., Jansa S.A. 2012. *Archboldomys* (Muridae: Murinae) reconsidered: a new genus and three new species of shrew mice from Luzon Island, Philippines. American Museum Novitates 3754:1–60.

Balete D.S., Rickart E.A., Heaney L.R., Jansa S.A. 2015. A new species of *Batomys* (Muridae, Rodentia) from southern Luzon Island, Philippines. Proceedings of the Biological Society of Washington 128:22–39.

Bouckaert R., ET AL. 2019. BEAST 2.5: an advanced software platform for Bayesian evolutionary analysis. PLoS Computational Biology 15:1–28.

Bouckaert R.R., Heled J., Kühnert D., Vaughan T.G., Wu C.H., Xie D., Suchard M.A., Rambaut A., Drummond A.J. 2014. BEAST 2: a software platform for Bayesian evolutionary analysis. PLoS Computational Biology 10:1–7.

Brown J.C. 1972. The description of mammals. 1. The external characters of the head. Mammal Review 1:151–168.

Brown J.C., Yalden D.W. 1973. The description of mammals. 2. Limbs and locomotion of terrestial mammals. Mammal Review 3:107–134.

Burgin C.J., Colella J.P., Kahn P.L., Upham N.S. 2018. How many species of mammals are there? Journal of Mammalogy 99:1–14.

Dickerson R.E., Merrill E.D., McGregor R.C., Schultze W., Taylor E.H., Herre A.W.C.T. 1928. Distribution of life in the Philippines. Monographs of the Philippine Bureau of Science 21:1–322.

Dmitriev D.A., Rakitov R.A. 2008. Decoding of superimposed traces produced by direct sequencing of heterozygous indels. PLoS Computational Biology 4:1–10.

Drummond A.J., Ho S.Y.W., Phillips M.J., Rambaut A. 2006. Relaxed phylogenetics and dating with confidence. PLoS Biology 4:699–710.

Edgar R.C. 2004. MUSCLE: multiple sequence alignment with high accuracy and high throughput. Nucleic Acids Research 32:1792–1797.

Elera C. De. 1915. Contribucion a la fauna Filipina. Universidad de Santo Tomás, Manila, Philippines.

Fernando E.S., Suh M.H., Lee J., Lee D.K. 2008. Forest formations of the Philippines. ASEAN-Korea Environmental Cooperation Unit, Seoul, Korea.

Gillespie R.G. 2004. Community assembly through adaptive radiation in Hawaiian spiders. Science 303:356–359.

Givnish T.J., Millam K.C., Mast A.R., Paterson T.B., Theim T.J., Hipp A.L., Henss J.M., Smith J.F., Wood K.R., Sytsma K.J. 2009. Origin, adaptive radiation and diversification of the Hawaiian lobeliads (Asterales: Campanulaceae). Proceedings of the Royal Society B 276:407–416.

Gu X., Fu Y.X., Li W.H. 1995. Maximum likelihood estimation of the heterogeneity of substitution rate among nucleotide sites. Molecular Biology and Evolution 12:546–557.

Hall, R. 2013. The palaeogeography of Sundaland and Wallacea since the Later Jurassic. Journal of Limnology 72:1–17.

Heaney L.R. 1986. Biogeography of mammals in SE Asia: estimates of rates of colonization, extinction and speciation. Biological Journal of the Linnean Society 28:127–165.

Heaney L.R. 2004. Conservation biogeography in oceanic archipelagoes. In: Heaney L.R., Lomolino M.V., editors. Frontiers of biogeography: new directions in the geography of nature. Sinauer Associates, Sunderland, Massachusetts, USA, 345–360.

Heaney L.R., ET AL. 1998. A synopsis of the mammalian fauna of the Philippine Islands. Fieldiana Zoology 88:1–61.

Heaney L.R., Balete D.S., Duya M.R.M., Duya M.V., Jansa S.A., Steppan S.J., Rickart E.A. 2016a. Doubling diversity: a cautionary tale of previously unsuspected mammalian diversity on a tropical oceanic island. Frontiers of Biogeography 8:1–19.

Heaney L.R., Balete D.S., Rickart E.A. 2016b. The mammals of Luzon Island. Johns Hopkins University Press, Baltimore, Maryland, USA.

Heaney L.R., Balete D.S., Rickart E.A., Alviola P.A., Duya M.R.M., Duya M.V., Veluz M.J., VandeVrede L., Steppan S.J. 2011. Seven new species and a new subgenus of forest mice (Rodentia: Muridae: *Apomys*) from Luzon Island. Fieldiana Life and Earth Sciences 2:1–60.

Heaney L.R., Balete D.S., Rickart E.A., Veluz M.J., Jansa S.A. 2009. A new genus and species of small "tree-mouse" (Rodentia, Muridae) related to the Philippine giant cloud rats. Bulletin of the American Museum of Natural History 331:205–229.

Heaney L.R., Balete D.S., Veluz M.J., Steppan S.J., Esselstyn J.A., Pfeiffer A.W., Rickart E.A. 2014. Two new species of Philippine forest mice (*Apomys*, Muridae, Rodentia) from Lubang and Luzon Islands, with a redescription of *Apomys*. Proceedings of the Biological Society of Washington 126:395–413.

Heaney L.R., Kyriazis C.C., Balete D.S., Rickart E.A., Bates J.M. 2021. A new species of *Bullimus* (Muridae, Rodentia) from southern Luzon Island, Philippines. Proceedings of the Biological Society of Washington 134:131–148.

Heaney L.R., Kyriazis C.C., Balete D.S., Steppan S.J., Rickart E.A. 2018. How small an island? Speciation by endemic mammals (*Apomys*, Muridae) on an oceanic Philippine island. Journal of Biogeography 45:1675–1687.

Heaney L.R., Tabaranza B.R. Jr., Rickart E.A., Balete D.S., Ingle N.R. 2006. The mammals of Mt. Kitanglad Nature Park, Mindanao, Philippines. Fieldiana Zoology 112:1–63.

Hollister N. 1913. A review of the Philippine land mammals in the United States National Museum. Proceedings of the United States National Museum 46:299–341.

Hoogstraal H. 1951. Philippine zoological expedition 1946–1947: narrative and itinerary. Fieldiana Zoology 33:1–86.

Jansa S.A., Barker F.K., Heaney L.R. 2006. The pattern and timing of diversification of Philippine endemic rodents: evidence from mitochondrial and nuclear gene sequences. Systematic Biology 55:73–88.

Justiniano R., Schenk J.J., Balete D.S., Rickart E.A., Esselstyn J.A., Heaney L.R., Steppan S.J. 2015. Testing diversification models of endemic Philippine forest mice (*Apomys*) with nuclear phylogenies across elevational gradients reveals repeated colonization of isolated mountain ranges. Journal of Biogeography 42:51–64.

Kimura Y., Hawkins M.T.R., McDonough M.M., Jacobs L.L., Flynn L.J. 2015. Corrected placement of *Mus* - *Rattus* fossil calibration forces precision in the molecular tree of rodents. Scientific Reports 5:1–9.

Kummer D.M. 1992. Deforestation in the postwar Philippines. Ateneo de Manila University Press, Manila, Philippines.

Kyriazis C.C., Bates J.M., Heaney L.R. 2017. Dynamics of genetic and morphological diversification in an incipient intra-island radiation of Philippine rodents (Muridae: *Bullimus*). Journal of Biogeography 44:2585–2594.

Lanfear R., Calcott B., Ho S.Y.W., Guindon S. 2012. PartitionFinder: combined selection of partitioning schemes and substitution

models for phylogenetic analyses. Molecular Biology and Evolution 29:1695–1701.

Lecompte E., Aplin K.P., Denys C., Catzeflis F., Chades M., Chevret P. 2008. Phylogeny and biogeography of African Murinae based on mitochondrial and nuclear gene sequences, with a new tribal classification of the subfamily. BMC Evolutionary Biology 8:1–21.

Mahler D.L., Revell L.J., Glor R.E., Losos J.B. 2010. Ecological opportunity and the rate of morphological evolution in the diversification of greater Antillean anoles. Evolution 64:2731–2745.

Mallari N.A.D., Tabaranza B.R. Jr., Crosby M.J. 2001. Key conservation sites of the Philippines: a Haribon Foundation & Birdlife International directory of important bird areas. Bookmark, Inc., Makati City, Philippines.

Marcy A.E., Guillerme T., Sherratt E., Rowe K.C., Phillips M.J., Weisbecker V. 2020. Australian rodents reveal conserved cranial evolutionary allometry across 10 million years of murid evolution. The American Naturalist 196:755–768.

Mearns E.A. 1905. Descriptions of new genera and species of mammals from the Philippine Islands. Proceedings of the United States National Museum 28:425–460.

Miller M.A., Pfeiffer W., Schwartz T. 2010. Creating the CIPRES Science Gateway for inference of large phylogenetic trees. 2010 Gateway Computing Environments Workshop, GCE 2010.

Mines and Geosciences Bureau. 2010. Geology of the Philippines. 2nd ed. Mines and Geosciences Bureau, Quezon City, Philippines.

Moura M.R., Jetz W. 2021. Shortfalls and opportunities in terrestrial vertebrate species discovery. Nature Ecology & Evolution 5:631–639.

Musser G.G. 1981. A new genus of arboreal rat from West Java, Indonesia. Zoologische Verhandelingen 189:3–35.

Musser G.G. 1982a. Results of the Archbold Expeditions No. 110: *Crunomys* and the small-bodied shrew rats native to the Philippine Islands and Sulawesi (Celebes). Bulletin of the American Museum of Natural History 174:1–95.

Musser G.G. 1982b. Results of the Archbold Expeditions No. 108: the definition of *Apomys*, a native rat of the Philippine Islands. American Museum Novitates 2746:1–43.

Musser G.G., Heaney L.R. 1992. Philippine rodents: definitions of *Tarsomys* and *Limnomys* plus a preliminary assessment of phylogenetic patterns among native Philippine murines (Murinae, Muridae). Bulletin of the American Museum of Natural History 211:1–138.

Musser G.G., Heaney L.R., Tabaranza B.R. Jr. 1998. Philippine rodents: redefinitions of known species of *Batomys* (Muridae, Murinae) and description of a new species from Dinagat Island. American Museum Novitates 3237:1–51.

Ogilvie H.A., Bouckaert R.R., Drummond A.J. 2017. StarBEAST2 brings faster species tree inference and accurate estimates of substitution rates. Molecular Biology and Evolution 34:2101–2114.

Rabor D.S. 1966. A report on the zoological expeditions in the Philippines for the period 1961–1966. Silliman Journal 13:604–616.

R Core Team. 2018. R: a language and environment for statistical computing. R Foundation for Statistical Computing, Vienna, Austria.

Rickart E.A., Balete D.S., Timm R.M., Alviola P.A., Esselstyn J.A., Heaney L.R. 2019. Two new species of shrew-rats (*Rhynchomys*: Muridae: Rodentia) from Luzon Island, Philippines. Journal of Mammalogy 100:1112–1129.

Rickart E.A., Heaney L.R., Tabaranza B.R. Jr. 2003. A new species of *Limnomys* (Rodentia: Muridae: Murinae) from Mindanao Island, Philippines. Journal of Mammalogy 84:1443–1455.

Rowe K.C., Achmadi A.S., Esselstyn J.A. 2016. Repeated evolution of carnivory among Indo-Australian rodents. Evolution 70:653–665.

Rowe K.C., Achmadi A.S., Fabre P., Schenk J.J., Steppan S.J., Esselstyn J.A. 2019. Oceanic islands of Wallacea as a source for dispersal and diversification of murine rodents. Journal of Biogeography 46:2752–2768.

Rowe K.C., Aplin K.P., Baverstock P.R., Moritz C. 2011. Recent and rapid speciation with limited morphological disparity in the genus *Rattus*. Systematic Biology 60:188–203.

Rowsey D.M., Heaney L.R., Jansa S.A. 2018. Diversification rates of the "Old Endemic" murine rodents of Luzon Island, Philippines are inconsistent with incumbency effects and ecological opportunity. Evolution 72:1420–1435.

Rowsey D.M., Heaney L.R., Jansa S.A. 2019. Tempo and mode of mandibular shape and size evolution reveal mixed support for incumbency effects in two clades of island-endemic rodents (Muridae: Murinae). Evolution 73:1411–1427.

Sanborn C.C. 1952. Philippine zoological expedition, 1946–1947; mammals. Fieldiana Zoology 33:87–158.

Sanborn C.C. 1953. Mammals from Mindanao, Philippine Islands, collected by the Danish Philippine Expedition 1951–1952. Videnskabelige Meddelelser Dansk Naturhistorisk Forening 115:283–288.

Schenk J.J., Rowe K.C., Steppan S.J. 2013. Ecological opportunity and incumbency in the diversification of repeated continental colonizations by muroid rodents. Systematic Biology 62:837–864.

Schwarz G. 1978. Estimating the dimension of a model. The Annals of Statistics 6:461–464.

Sikes R.S., and the Animal Care and Use Committee of the American Society of Mammalogists. 2016. 2016 Guidelines of the American Society of Mammalogists for the use of wild mammals in research and education. Journal of Mammalogy 97:663–688.

Stamatakis A., Hoover P., Rougemont J. 2008. A rapid bootstrap algorithm for the RAxML web servers. Systematic Biology 57:758–771.

Steinbauer M.J., et al. 2016. Topography-driven isolation, speciation and a global increase of endemism with elevation. Global Ecology and Biogeography 25:1097–1107.

Taylor E.H. 1934. Philippine land mammals. Monographs of the Philippine Bureau of Science 30:1–548.

Valente L.M., Etienne R.S., Phillimore A.B. 2014. The effects of island ontogeny on species diversity and phylogeny. Proceedings of the Royal Society B 281:1–9.

Veron S., Haevermans T., Govaerts R., Mouchet M., Pellens R. 2019. Distribution and relative age of endemism across islands worldwide. Scientific Reports 9:11693.

Wallace A.R. 1880. Island life: or, the phenomena and causes of insular faunas and floras, including a revision and attempted solution of the problem of geological climates. Macmillan and Co., London, United Kingdom.

Walpole P. 2010. Figuring the forest figures: understanding forest cover data in the Philippines and where we might be proceeding. Environmental Science for Social Change 2010:1–37.

Whittaker R.J., Fernández-Palacios J.M., Matthews T.J., Borregaard M.K., Triantis K.A. 2017. Island biogeography: taking the long view of nature's laboratories. Science 357:1–7.

Yule G.U. 1924. A mathematical theory of evolution, based on the conclusions of Dr. J. C. Willis, F.R.S. Philosophical Transactions of the Royal Society B 213:21–87.

Yumul G.P., Dimalanta C.B., Maglambayan V.B., Marquez E.J. 2008. Tectonic setting of a composite terrane: a review of the Philippine island arc system. Geosciences Journal 12:7–17.

Submitted 8 April 2021. Accepted 13 May 2022.

Associate Editor was Kevin Rowe.

Appendix

Specimens examined for morphological analyses.—All specimens examined for phenetic and morphological analyses are currently housed at the Field Museum of Natural History, Chicago, Illinois (FMNH; *n* = 31). Specimens were collected from Luzon and Mindanao Islands, Republic of the Philippines.

Baletemys kampalili (*n* = 3).—See "new species" description above.

Limnomys bryophilus (*n* = 4).—Mindanao Island, Bukidnon Province, Mt. Katanglad Range, 18.5 km S, 4 km E Camp Phillips, elev. 2,250 m (8.1583°N, 124.85°E; FMNH 147977, 147978, 148181, 148182).

Limnomys sibuanus (*n* = 5).—Mindanao Island, Bukidnon Province, Mt. Katanglad Range, 16.5 km S, 4 km E Camp Phillips, elev. 2,250 m (8.175°N, 124.85°E; FMNH 147947, 148174); 18.5 km S, 4 km E Camp Phillips, elev. 2,250 m (8.1583°N, 124.85°E; FMNH 147949, 147950, 148175).

Rattus everetti (*n* = 20).—Luzon Island, Aurora Province, Dinalungan Municipality, 2.25 km S, 4.8 km E Mt. Anacuao Peak, elev. 740 m (17.73438°N, 121.9714°E; FMNH 209534); Cagayan Province, Peñablanca Municipality, 3 km N, 8.75 km W Mt. Cetacaeo Peak; elev. 730 m (17.73438°N, 121.9714°E; FMNH 216581); Camarines Sur Province, Caramoan National Park, 0.5 km S, 5 km E Port of Guijalo, elev. 50 m (13.73145°N, 123.91285°E; FMNH 203316); Lagonoy Munic, 0.8 km S, 1.5 km W Saddle Peak, elev. 550 m (13.7644°N, 123.644581°E; FMNH 198794); Mountain Province, 0.1 km E south peak Mt. Data, elev. 2,310 m (16.858881°N, 120.860781°E; FMNH 188465); Nueva Vizcaya Province, Quezon Municipality, 3.2 km N, 0.3 km W Mt. Palali peak, elev. 1,052 m (16.456719°N, 121.219489°E; FMNH 195063); Pampanga Province, Mabalacat Municipality, 1.8 km N, 6.25 km E Mt. Pinatubo peak, elev. 960 m (15.15145°N, 120.39784°E; FMNH 216376); Quezon Province, Mt. Banahaw, Barangay Lalo, elev. 620 m (14.05181°N, 121.47769°E; FMNH 191508); Quirino Province, Nagtipunan Municipality, Barangay Matmad, Sitio Mangitagud, Mungaio Mts, elev. 450 m (16.05625°N, 121.47769°E; FMNH 180430); Mindanao Island, Agusan del Norte Province, Mt. Hilong-Hilong, Barangay San Antonio (9.0967°N, 125.705°E; FMNH 191508); Bukidnon Province, Mt. Katanglad Range, 17 km S, 7 km E Baungon, elev. 1,550 m (8.17°N, 14.75°E; FMNH 146724); Compostela Valley Province, Maragusa Municipality, 2.75 km S, 0.5 km W Mt. Kampalili Peak, elev. 1,500 m (7.2942°N, 126.26067°E; FMNH 194798); Davao Oriental Province, 0.75 km S, 3.5 km W Mt. Hamiguitan, elev. 670 m (FMNH 191050, 191083); 1 km S, 10 km E Mt. Kampalili Peak, elev. 1,160 m (7.30138°N, 126.6874°E; FMNH 208831); South Cotabato Province, Polomoc Municipality, 0.6 km S, 0.4 km E Mt. Matutum Peak, elev. 1,850 m (6.35463°N, 125.0772°E; FMNH 206290); 1.4 km S, 0.55 km E Mt. Matutum Peak, elev. 1,450 m (6.3482°N, 125.07867°E; FMNH 206288); 3.35 km S, 0.25 km E, elev. 1,100 m (6.34163°N, 124.07555°E; FMNH 206291); Sultan Kudarat Province, Sen. Ninoy Aquino Municipality, Barangay Lagubang, 0.2 km N, 0.4 km E Mt. Daguma Peak, elev. 1,475 m (6.35348°N, 124.27327°E; FMNH 206145, 206305).

Tarsomys apoensis (*n* = 6).—Mindanao Island, Bukidnon Province, Mt. Katanglad Range, 1.6 km S, 4 km E Camp Phillips, elev. 1,900 m (8.175°N, 124.85°E; FMNH 147955, 147956); Mt. Katanglad Range, 18.5 km S, 4 km E Camp Phillips, elev. 2,250 m (8.1583°N, 124.85°E; FMNH 148176); Mt. Katanglad, Malaybalay (8.1°N, 124.9°E; FMNH 92802); Misamis Occidental Province, Mt. Malindang, Dapitan Peak (8.2167°N, 123.6334°E; FMNH 87594, 87595).

Tarsomys echinatus (*n* = 1).—Mindanao Island, South Cotabato Province, Polomoc Municipality, 2.1 km S, 0.25 km E Mt. Matutum Peak, elev. 1,250 m (6.34163°N, 125.07555°E; FMNH 206296).

Tarsomys sp. (*n* = 1).—Mindanao Island, Compostela Valley Province, Maragusan Municipality, 2 km S, 2 km W Mt. Kampalili peak, elev. 1,900 m (7.28685°N, 126.27525°E; FMNH 194803).

Specimens examined for molecular analyses.—Apomys datae: FMNH 167243, 188301; *Apomys hylocoetes*: FMNH 147871; *Archboldomys luzonensis*: USNM 473835, 573834, 573836; *Archboldomys maximus*: FMNH 193522, 193526, 193944; *Baletemys kampalili*: FMNH 194802, 194804, 208788; *Batomys granti*: FMNH 188321, 188322; *Bullimus luzonicus*: FMNH 167310; *Carpomys phaeurus*: FMNH 198723; *Chrotomys silaceus*: FMNH 193727, 193734; *Chrotomys whiteheadi*: FMNH 188360, 188458, 188462, 193747; *Crateromys schadenbergi*: 193750, 198871; *Crunomys celebensis*: NMV C37047; *Crunomys melanius*: FMNH 147105, 191498, 191499; *Crunomys suncoides*: FMNH 147942; *Kadarsanomys sodyi*: MZB 34728; *Leopoldamys sabanus*: FMNH 168675; *Limnomys bryophilus*: FMNH 147970, 147972, 147974, 147977, 148180, 148182; *Limnomys sibuanus*: FMNH 147944, 147945, 147946, 147947, 148174, 206281; *Maxomys hellwaldii*: MVZ 225768; *Maxomys panglima*: FMNH 196044, 196045, KU 165356, 165456; *Musseromys beneficus*: FMNH 198715; *Palawanomys furvus*: 196055, 196056, 196057; *Phloeomys cumingi*: USNM 573935, 573936; *Rattus everetti*: FMNH 142352, 142353, 146722, 183433, 191010, 191502, 191506, 194798, 194800, 194801, 196061, 198875, 205501, 206149, 206156, 206421, 216309; *Rattus exulans*: FMNH 198876, 198877, NK80010; *Rattus facetus*: MVZ225821; *Rattus fuscipes*: Chimera ABTC 51715/08616/GI02R01; *Rattus hoffmanni*: MVZ 225736; *Rattus leucopus*: KU 160770; *Rattus losea*: ABTC 118627; *Rattus lutreolus*: ABTC 51720; *Rattus mindorensis*: FMNH 222185, 222189, 222981, 222982; *Rattus morotaiensis*: ASAM85; *Rattus norvegicus*: MX 71, PL 6767, S1 S2; *Rattus novaeguineae*: ABTC 46853; *Rattus praetor*: Chimera USNM 580077/ABTC 47273/ABTC 51664/ABTC 47252; *Rattus rattus*: MVZ 08242, MG-09, NP054PuP, NP103KK, SP63, Chimera CACGA65/ASK3695; *Rattus sordidus*: Chimera ABTC 51622/ABTC 51664/RAT176; *Rattus* sp. Sibuyan Island: FMNH 135719, 135720, 145719, 145720, 145727, 145735, 145736; *Rattus tanezumi*: FMNH 167497, 167959, 167960, MVZ 186527, R120722; *Rattus tiomanicus*: FMNH 198786, 198788, 198789; *Rattus tunneyi*: Chimera ABTC 51688/ABTC 08815/Rat132; *Rattus verecundus*: Chimera SAMA 43425/ABTC 47140; *Rattus villosissimus*: Chimera SAMA 00549/ABTC 08439; *Rhynchomys soricoides*: FMNH 198786 198788 198789; *Soricomys kalinga*: FMNH 167304, 170967, 175557, 175558, 175559, 175721; *Soricomys leonardocoi*: FMNH 190963, 190970, 190974, 190982; *Soricomys montanus*: FMNH 185907, 185908, 185909, 185910; *Soricomys musseri*: FMNH 185907, 185908, 185909, 185910; *Sundamys muelleri*: UMMZ 174438, 174440; *Tarsomys apoensis*: FMNH 147954, 147955, 147956, 148176, 148177, 148178; *Tarsomys echinatus*: FMNH 206296; *Tarsomys* sp.: FMNH 194803, 208755.